IEEE Access
Multidisciplinary | Rapid Review | Open Access Journal

Received March 22, 2021, accepted April 7, 2021, date of publication April 13, 2021, date of current version April 21, 2021.

Digital Object Identifier 10.1109/ACCESS.2021.3073020

Recent Achievements in Model Predictive Control Techniques for Industrial Motor: A Comprehensive State-of-the-Art

MAHMOUD F. ELMORSHEDY[1], (Member, IEEE), WEI XU[2], (Senior Member, IEEE), FAYEZ F. M. EL-SOUSY[3], (Member, IEEE), MD. RABIUL ISLAM[4], (Senior Member, IEEE), AND ABDELSALAM A. AHMED[1]

[1]Electrical Power and Machines Engineering Department, Faculty of Engineering, Tanta University, Tanta 31511, Egypt
[2]State Key Laboratory of Advanced Electromagnetic Engineering and Technology, Huazhong University of Science and Technology, Wuhan 430074, China
[3]Electrical Engineering Department, College of Engineering, Prince Sattam Bin Abdulaziz University, Al-Kharj 11942, Saudi Arabia
[4]School of Electrical, Computer and Telecommunications Engineering, University of Wollongong, Wollongong, NSW 2522, Australia

Corresponding author: Wei Xu (weixu@hust.edu.cn)

This work was supported in part by the National Natural Science Foundation of China under Grant 51877093, in part by the National Key Research and Development Program of China under Grant YS2018YFGH000299, and in part by the Key Technical Innovation Program of Hubei Province under Grant 2019AAA026.

ABSTRACT Model predictive control (MPC), manly based on a direct use of an explicit and identifiable model, has been widely used in controller design in different applications both by academia and industry. The reason for such popularity is due to its strong ability for providing high performance electric drive systems, as highly recognized as the most reliable control approach compared with field-oriented control (FOC) and direct torque control (DTC). In general, the MPC has numerous features and advantages, such as direct switching states to the converter without any modulation, online optimization with multivariable control, low current total harmonic distortion, low switching loss, *etc*. The aim of this paper is to provide a comprehensive review for major development and achievements of the recent progress on the MPC for electrical machines and drives. This review begins with the innovative topologies and operating principles of fundamental MPC, and ends to summary on different advanced MPC algorithms. Typical MPC techniques have been fully adopted to enhance the drive performance of the electrical drives, mainly including finite-set model predictive control (FS-MPC) based on tuning weighting factors, without weighting factors, maximum torque per ampere, low number of switching vectors, and multi voltage vectors in one sample period. Finally, great attention has been paid to the discussion of the new trends and future research topics.

INDEX TERMS Model predictive control (MPC), finite-set MPC (FS-MPC), weighting less FS-MPC, efficient MPC, maximum torque per ampere (MTPA), field-oriented control (FOC), direct torque control (DTC).

NONCULTURE

ABBREVIATIONS

AOF	Aggregation of functions
BLDC	Blushless DC machine
CCS	Continuous control set
DCC	Duty cycle control
DPSC	Direct predictive speed control
DSP	Digital signal processor
DSVM	Discrete space vector modulation
DTC	Direct torque control
EWF	Eliminating weighting factor
FCS	Finite control set
FOC	Field-oriented control
FPGA	Field programmable gate array
GPIO	Generalized proportional-integral observer
IM	Induction machine
LIM	Linear induction machine
MPC	Model predictive control
MPCC	Model predictive current control
MPDAC	Model predictive direct angle control
MPDTC	Model predictive direct torque control

The associate editor coordinating the review of this manuscript and approving it for publication was Giambattista Gruosso.

MPFC	Model predictive flux control
MTPA	Maximum torque per ampere
PMSM	Permanent magnetic synchronous machine
PWM	Pulse width modulation
RMS	Root-mean-square
SRM	Synchronous reluctance machine
SV	Space vector
THD	Total harmonic distortion
VSI	Voltage source inverter
VV	voltage vectors

PARAMETERS AND CONSTANTS

i_s	Stator current
T_e	Electromagnetic torque
V_{dc}	DC-link voltage
u_d	d-axis voltage
u_q	q-axis voltage
u_α	α-axis voltage
u_β	β-axis voltage
W	Weighting factor
ψ_s	Stator flux-linkage
ψ_r	Rotor flux-linkage
τ_r	Rotor time constant

VARIABLES AND FUNCTIONS

g	Cost function
G_{0i}	Dynamic cost function
g_{1i}	Torque error at every voltage vector
g_{1max}	Maximum value of g_{1i}
g_{1min}	Minimum value of g_{1i}
g_{2i}	Stator flux error at every voltage vector
g_{2max}	Maximum value of g_{2i}
g_{2min}	Minimum value of g_{2i}
V_i	Voltage vector

I. INTRODUCTION

From the past three decades, the model predictive control (MPC) has been paid more attention by both academia and industry. At the end of 1970s, the theory of MPC was originally developed [1]. In 1983, the MPC was used in power electronics [2]. Since 2000, the great increase of computation capability for the microprocessors has accelerated wide applications of the MPC in electric drives and power converter systems gradually [3]–[7]. Compared to the field-oriented control (FOC) and direct torque control (DTC) methods, the MPC is considered as the most reliable control approach in the electric drive applications [8], [9]–[13].

In general, the MPC has some typical advantages such as easy to understand, online optimization, inclusion of different constraints and nonlinearities, low current distortion, small switching losses, and so on [14]–[18]. However, as every coin has two sides, the MPC also suffers a few drawbacks compared to the FOC or DTC, like more variable switching frequency, higher torque and flux ripple, higher total harmonic distortion in the current, and so on. Therefore, some modifications and improvements for the MPC have been proposed and then developed by the researchers in order to solve the aforementioned problems [19]. Regarding to the implementation of the MPC, different types of control platforms have been used like digital signal processors (DSPs) [20]–[22], dSPACE semi-physical simulation system [12], [23], [24], field programmable gate arrays (FPGAs) [25]–[28], *etc*. These control platforms are based on the use of microprocessor units with exponentially increasing calculation ability. Besides, they can guarantee the requirements of different applications, the use of multi-level converters and multiple-step predictions [11], [29]–[31]. One important thing, the MPC is not dependent on the machine type. Hence, it is flexibly applicable for all kinds of electrical machines (like rotary machines or linear machines), including induction machines (IMs), synchronous reluctance machines (SRMs), permanent magnet synchronous machines (PMSMs), blushless DC machines (BLDCs), multiphase machines, linear induction machines (LIMs) [19], [22], [32]–[37], and so on.

The working principle of the MPC is based on selecting the best switching vector, which leads to the lower value of the cost function [38]. For the three-phase two-level voltage source inverter (3-ph 2-L VSI), there are eight voltage vectors (VVs) resulting from the combinations of the switching state for each switch. Among them, there are six active VVs (U1-U6) and two zero VVs (U0, U7). These six active VVs are shifted by $\pi/3$ from each other, and the vector plane is divided into six sectors, as shown in Fig. 1.

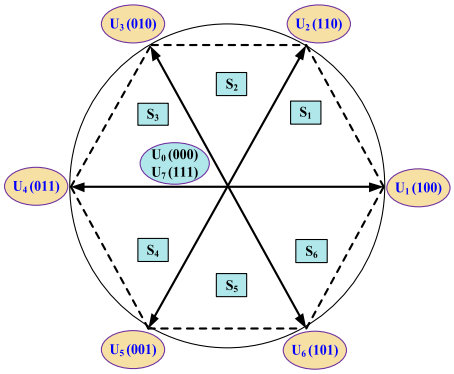

FIGURE 1. Switching vectors of the three-phase two-level voltage source inverter.

The process of the MPC is composed of three paradigms named as estimation step, prediction step, and cost function design step. According to the designed cost function, the states used in both estimation and prediction are determined [39]. Regarding to the finite control set model predictive control (FCS-MPC), two types are used to control the performance of the electric drive: the first one is finite control set model predictive current control (FCS-MPCC) [40], [41], and the second one is finite control set model predictive direct torque control (FCS-MPDTC) [14], [15].

Detailed comparisons between FS-MPCC and FS-MPDTC are presented experimentally for the rotary induction machines (RIMs) in [32]. At this instance, the usage of the MPC for electric machines and power converters is considered as a well-established technology in the theoretical research stages. However, a lot of efforts are needed to transfer such technology to the industrial applications [35], [43]–[46]. Therefore, this paper presents a comprehensive review for the recent advancements of the MPC algorithms, such as different types of the MPC, conventional finite control set model predictive control (FCS-MPC), finite control set model predictive control with optimum duty ratio calculation (FCS-MPC-I), finite control set model predictive control with maximum torque per ampere (FCS-MPC-II), continuous control set model predictive control (CCS-MPC), weighting less MPC, and so on, as illustrated in Fig. 2.

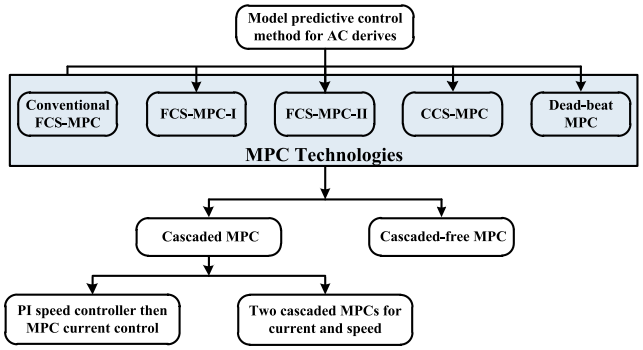

FIGURE 2. Advanced MPC strategies for AC drives.

Moreover, another objective of this review is to extend the limitation of existing publications on the promising MPC for electric drives. Therefore, it includes the available advantages of each control method as well as shortcomings of the existing review on MPC, as well as the relevant recommendations for the future work. By full studying the available literatures on the MPC for electric drives, an elaborate presentation on the state of different kinds of MPC for different machines is outlined and clarified in details.

This paper is organized as follows. The different technologies of the model predictive control are discussed firstly in the introduction section. Then, a comparison between finite and continuous set MPC is presented in Section II. This section includes the main difference between both of them, mathematical equations and how to implement. After that, the improvements for the MPC which leads to less ripples based on the optimum duty ratio are provided in Section III. Furthermore, this section is supported by full experimental results. The weighting factor is considered a big challenge for the MPC, thus Section IV focuses on the different techniques of tuning weighting factor, and some new methods are applied to remove the use of weighting factors. Section V discusses the maximum torque per ampere based on MPC which is an important method to increase the drive system efficiency. Moreover, Section VI is added to present the direct speed MPC, which is one emerging research area for the MPC. Also, the stability of the MPC is presented in Section VII. Finally, the conclusion with the future research trends is added in Sections VIII.

II. FINITE AND CONTINOUS CONTROL SETS MPC

A. CONCEPT AND PRINCIPLES

Generally, for the electric drive control, there are two main groups of MPC that have been used by finite control set model predictive control (FCS-MPC) [18], [38], [47]–[50] and continuous control set model predictive control (CCS-MPC) [20], [37], [51], [52]–[55]. For the FCS-MPC, it is based on the selection of the optimal VV, which is directly applied to the gating signal of the VSI, and can minimize the designed cost function. Although the FCS-MPC has a good transient performance, it would result in high ripples in both torque and current. On the other hand, the CCS-MPC depends on voltage calculation (u_d^* and u_q^* or u_α^* and u_β^*) through minimizing the designed cost function for the reference tracking. Then, the gating signal of the VSI is determined through space vector pulse width modulation (SVPWM). Consequently, in one computational step, the FCS-MPC can solve the reference tracking and modulator problems. Hence, it is found the elimination on the SVPWM would bring some influences on the dynamic performance, ac-harmonics spectra, acoustic noise, inverter energy efficiency, *etc*. The general block diagram of the FCS-MPC and CCS-MPC is illustrated in Figs. 3. A comparative study between the FCS-MPC and CCS-MPC with optimum duty ratio and MTPA is fully presented in Section III.

As mentioned before, there are three steps for implementing the MPC in general. To illustrate these steps, the FCS-MPDTC is used as an example in this work, as proposed to overcome the disadvantages of large ripples in both electromagnetic torque and stator flux linkage, in comparison with the conventional DTC. Meanwhile, it is also presented to get one faster dynamics over the FOC.

B. DESIGN OF COST FUNCTION

In the FCS-MPDTC, the cost function is selected to minimize the electromagnetic torque, T_e, and the stator flux-linkage, ψ_s, as given by

$$g = \left|T_e^* - T_e\,(k+1)\right| + W\left|\psi_s^* - \psi_s\,(k+1)\right| \qquad (1)$$

where W is the weighting factor whose initial value can be determined by [56]. For designing the CCS-MPC, another technique has been used to find out the optimal applicable vector. This cost index is written in terms of the control input $u\,[k]$, as given by

$$J(k) = (x_s^*[k] - (Ax[k+1] + Bu[k]))^T W (x_s^*[k] - (Ax[k+1] + Bu[k])) \qquad (2)$$

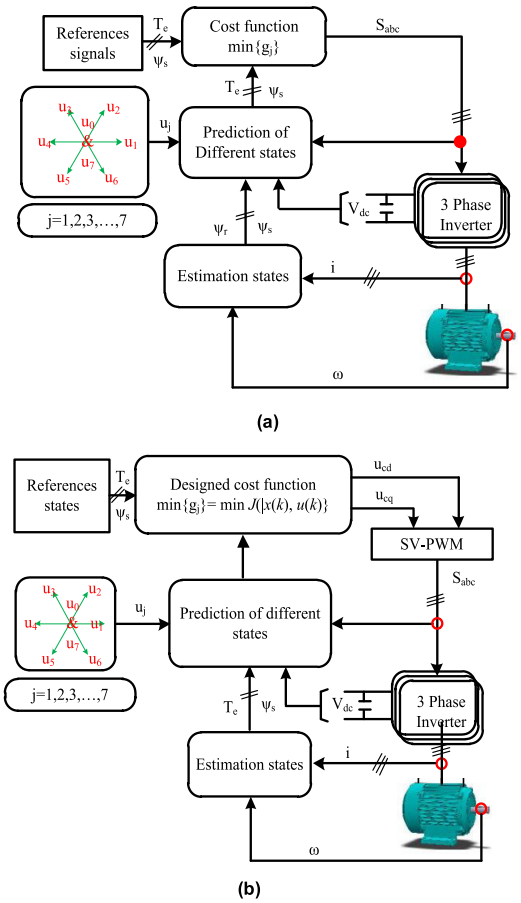

FIGURE 3. General block diagram of the MPC: (a) FCS-MPC and (b) CCS-MPC.

Let $u^*_{uc}(k)$ be the unconstrained optimizer of $J(k)$ in (2). Then, $u^*_{uc}(k)$ can be obtained by solving $\frac{\partial J(x(k),u(k))}{\partial u(k)} = 0$, as illustrated by

$$u^*_{uc}(k) = \left(B^T W B\right)^T \left(B^T W \begin{pmatrix} x^*_s\left(T^*_e, \lambda^*\right) \\ -Ax\left[k+2|k\right] \end{pmatrix}\right) \quad (3)$$

It is apparent that the optimizer $u^*_c(k)$ of the optimization problem in (3) is the same as the unconstraint $u^*_{uc}(k)$ if within the limits, i.e. $u^*_{uc}(k) \in U_c = \frac{1}{\sqrt{3}} V_{dc}$. The constrained input voltage $u^*_c(k)$ is constrained in dq-axis frame as

$$v^*_{cdq}(k) = U_c \frac{v^*_{ucdq}}{\sqrt{v^{*2}_{ucd} + v^{*2}_{ucq}}} \quad (4)$$

C. PREDICTION STEP

It can be noticed from the designed cost function in (1) that both T_e and ψ_s need to be predicted for the next step. Therefore, the prediction of the stator current is required for the second step prediction of the torque. Hence, the predicted states are described by [49]–[51]

$$\vec{\psi}_s(k+1) = \vec{\psi}_s(k) + T_s \vec{u}_s(k) - T_s R_s \vec{i}_s(k) \quad (5)$$

$$\vec{i}_s(k+1) = \left[1 - \frac{T_s}{\sigma}\left(R_s + \frac{R_r}{\tau_l^2}\right)\right] \vec{i}_s(k) + \frac{T_s}{\sigma}\left(\vec{u}_s(k) + \frac{1}{\tau_r \tau_l}\vec{\psi}_r(k) + j\frac{\omega_r}{\tau_l}\vec{\psi}_r(k)\right) \quad (6)$$

$$T_e(k+1) = \frac{3}{2}\frac{\pi}{\tau}\vec{\psi}_s(k+1) \otimes \vec{i}_s(k+1) \quad (7)$$

where $\sigma = \left(L_s - \frac{L_m^2}{L_r}\right)$, $\tau_r = \frac{L_r}{R_r}$ and $\tau_l = \frac{L_r}{L_m}$. T_s is the sampling period, $u_1(k)$ one of the voltage vectors ($u_1(0, 1, 2, \ldots, 7)$) as shown in Fig. 1. From this picture, it is considered as an appropriated control action that can make the system variables much close to their references (T^*_e and ψ^*_s).

D. ESTIMATION STEP

For the FCS-MPTC, the rotor flux is estimated for current prediction step. From (5) and (6), it can be observed that the stator and the rotor flux-linkages are needed in the prediction step, as estimated by

$$\vec{\psi}_r(k) = \frac{\left[R_r T_s L_m \vec{i}_s(k) - jT_s L_r \omega_r \vec{\psi}_r(k) + L_r \vec{\psi}_r(k-1)\right]}{\left[L_r + R_r T_s\right]} \quad (8)$$

$$\vec{\psi}_s = \frac{L_m}{L_r}\left(\vec{\psi}_r - \left(L_m - \frac{L_r L_s}{L_m}\right)\vec{i}_s\right) \quad (9)$$

where i_s can be obtained from the measured three-phase current, and then transformed to the vector coordinates. In the same way, for the CCS-MPC, the load torque should be estimated for the speed prediction step. The optimal control input T^*_e, minimizing the cost index (2) in each time step, is obtained from $\frac{d}{dT^*_e} J_m = 0$, as calculated by

$$T^*_e = \frac{J}{pT_{sw}}\left(e_{ms}\left[k+1\right] + \frac{B_m T_{sw}}{J} x_m\left[k+1\right] + \frac{pT_{sw}}{J}\hat{T}_L\left[k\right]\right) \quad (10)$$

where $e_{ms}[k+1|k] = x^*_{ms}[k+1] - x_m[k+1]$ is the speed error, and $\hat{T}_L[k]$ the estimated load torque. In this case, the reference speed should be reduced to the point so that the maximum admissible torque is equal to $\hat{T}_L[k]$, i.e. the rotor speed that satisfies the condition of (2) is considered as the limited speed reference (3) [20], as depicted by

$$T^*_{e\_max}\left(\omega^*_r\right) \le \hat{T}_L\left[k\right] \quad (11)$$

$$\omega^*_r = \omega_r \quad (12)$$

As seen from (10), the load torque $\hat{T}_L$ is mandatorily estimated to be properly compensated by the control strategy. The standard Kalman Filter is one robust technique for the load torque estimation [20]. To summarize the steps and processes of the FS-MPDTC, one flow chart is presented in Fig. 4, to illustrate the operation process. Moreover, the block diagram of the speed control for the IM based on the FS-MPDTC is illustrated in Fig. 5.

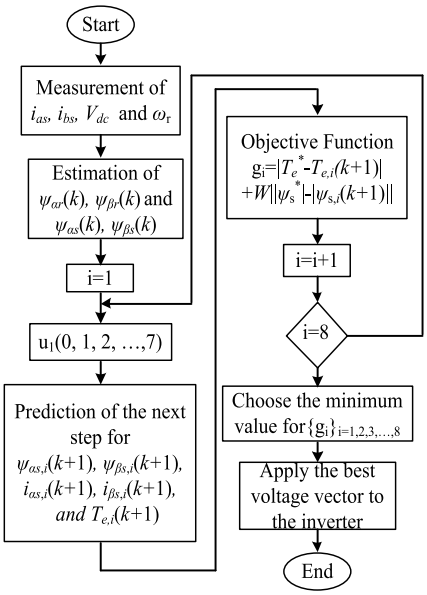

FIGURE 4. Flowchart diagram of the FCS-MPDTC for the IM.

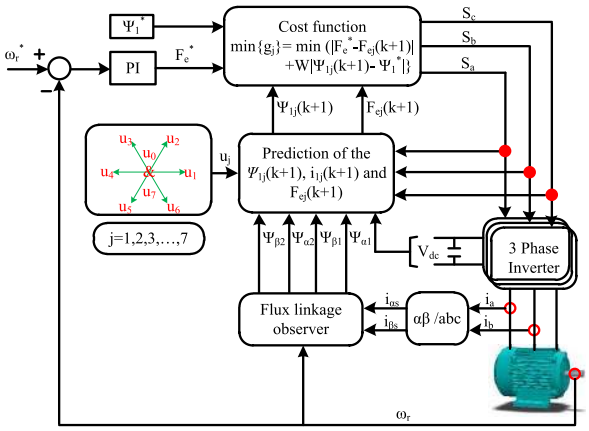

FIGURE 5. Block diagram of the conventional FCS-MPDTC for the IM.

III. MPC WITH OPTIMUM DUTY RATIO CALCULATION

A. FCS-MPC WITH SEPARATE OPTIMUM DUTY RATIO

In the previous section, only the best switching voltage vector is applied in the whole sample period. Hence, some relatively high ripples are presented in both stator and torque. Therefore, to overcome these problems, many papers have fouced on the determination of the optimum switching instant [5], [7], [60]–[68]. In [7], the optimal voltage vector is selected based on the principle of stator flux error minimization whose switching instant is optimized rather than being in the beginning of each control period. Two variants of model predictive flux control (MPFC) are presented here: the first one is concerning on low switching frequency, and the second one is focusing more on the steady-state performance by introducing switching instant optimization. By providing the optimum switching instant, some reduction on torque ripples, flux ripples, and current total harmonic distoration (THD) can be observed. In [65], a Lyaupnov-based FCS-MPDTC for the PMSM is proposed. The Lyapunov theory and the FCS prediction are mixed to minimize the torque ripple where the Lyapunov function is utilized as the main part of the cost function to estimate the duty cycle of each voltage vector. Hence, the optimum voltage vector and its duty cycle are obtained. The proposed control method can realize a fixed switching frequency, a small sampling frequency, and torque ripple minimization. Finally, both simulation and experiments validate the strong drive performance of the proposed control. Both torque and current ripples can be significantly reduced when compared to the torque control with standard FCS-MPC.

Moreover, a new predictive torque control (PTC) based on discrete space vector modulation (DSVM) for IM is proposed in [67]. This DSVM has the feature of increasing the number of voltage vectors that leads to high computational burden. This problem is avoided by reducing the number of admissible voltage vectors based on the switching table of the conventional DTC. This new control method can gurantee lower sampling frequency by three times compared to the conventional PTC. On the other hand, it still has the same behaviour in terms of stator current THD, dynamic torque response with the same switching frequency, and torque and flux ripple. Moreover, the low sampling frequency of the proposed algorithm makes it suitable for industries to use low-cost hardware or perform a high computational analysis.

Further, a novel duty cycle control (DCC) method is proposed in [61] to reduce flux and torque ripples where the appropriate active voltage vector (VV) is firstly selected based on the principles of the conventional DTC. Then, a zero VV is inserted with the selected one to generate a new candidate VVs with different duty cycles. The new VVs can be calculated by

$$\vec{V}_i = \left(\frac{i}{n}\right) * \vec{V}_{act} + \left(\frac{n-i}{n}\right) * \vec{V}_{0,7} \quad (i = 1, \ldots, n) \quad (13)$$

After that, the FCS-MPC technique is employed to select the best VV among the new candidates to reduce flux and torque errors. The block diagram of the proposed DCC method is shown in Fig. 6. The experimental results have verified the excellent performance and the superiority of the DCC over those of the classical DTC and conventional MPC methods. In addition, lower torque and flux ripples have been achieved and almost a fixed switching frequency for all speed ranges can be got.

Finally, the optimum voltage vector and its duty cycle can be implemented in different ways. But in general, all of these ways can be classified into two types during the implementation. The first one is to determine the optimum voltage vector and then calculate the optimum duty ratio for this voltage vector. The diagram is shown in Fig. 7.

B. FCS-MPC WITH OPTIMIZATION OF VOLTAGE AND DURATION SIMULTANEOUSLY

The FCS-MPC in [59] can compute optimal modulation factors for all nonzero vectors following the deadbeat criteria,

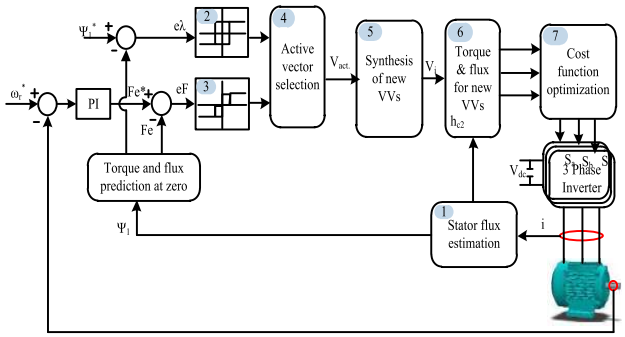

FIGURE 6. Block diagram of the DCC for the IM [61].

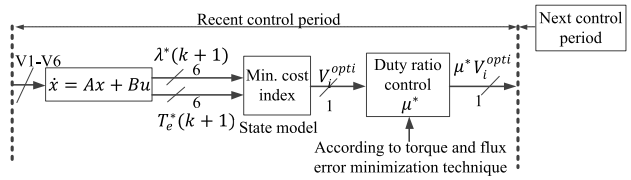

FIGURE 7. FCS-MPC with separate duty cycle control.

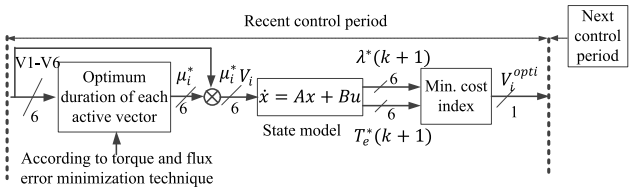

FIGURE 8. FCS-MPC with optimization of voltage.

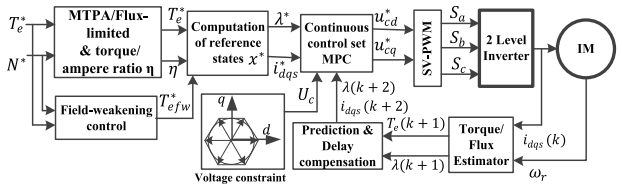

FIGURE 9. Main configurations of the CCS-MPC of ac drives.

and then obtains the optimal control vector with the optimal modulation factor considering a cost index penalizing torque and flux tracking error separately, as illustrated in Fig. 8.

C. CCS-MPC WITH SEPEARATE OPTIMUM DUTY RATIO

Compared to the idea of a separate optimum duty ratio as presented for FCS-MPC in [69], the CCS-MPC can be implemented by inserting the optimum duty ratio. In this case, it consists of four main stages: (1) Computation of the reference state for a given torque, (2) Calculation of flux reference in field-weakening region, (3) CCS-MPC design considering the voltage and current constraints, and finally (4) Modulation technique. These stages are fully illustated in Fig. 9. Meanwhile, Flowcharts of two cascaded FCS-MPC and cascaded CCS-MPC for speed and current control of ac drives f are shown in Fig. 10(a) and 10(b), respectively.

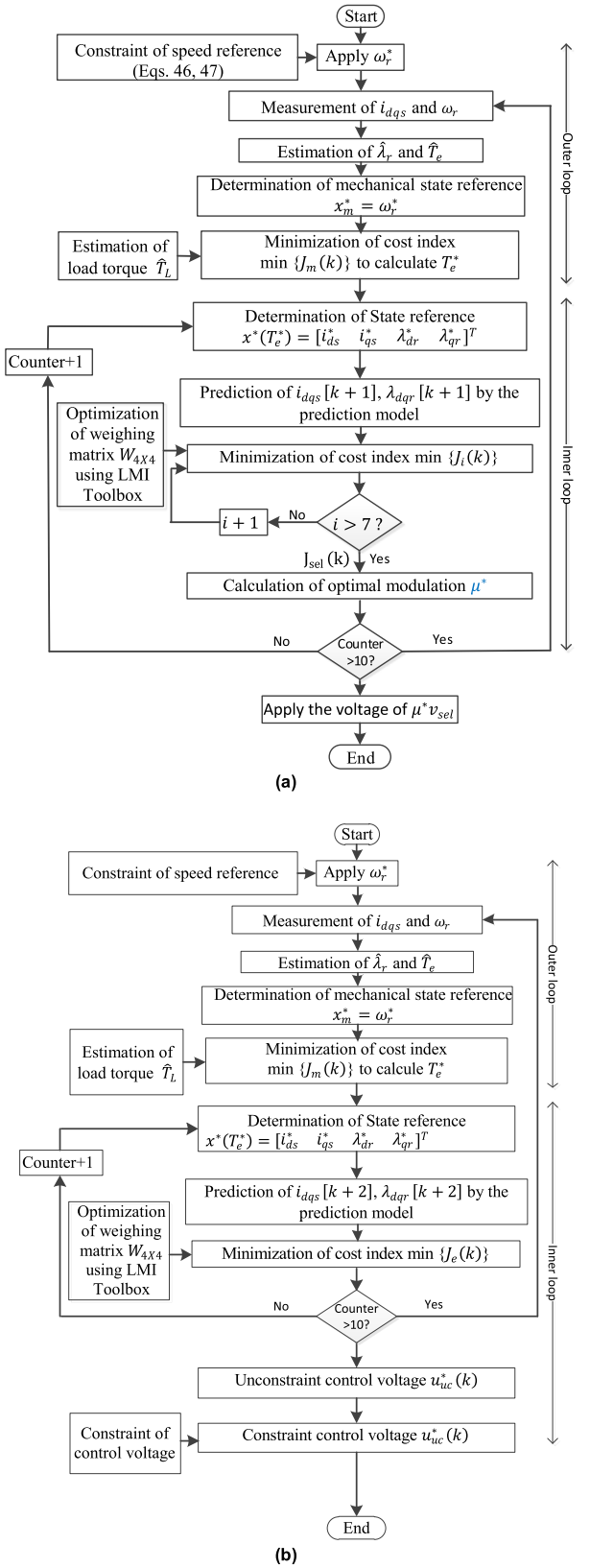

FIGURE 10. Flowchart of two cascaded MPCs for speed and current control of ac drives: (a) cascaded FCS-MPC and (b) cascaded CCS-MPC.

TABLE 1. Main parameters for the IM and drive.

Item	Symbol	Value
DC-bus volt (V)	v_{dc}	500
Rated current (A)	I_{rms}	14.2/8.2
Stator resistance (Ω)	R_s	1.77
Rotor resistance (Ω)	R_r	1.275
Stator inductance (H)	L_s	0.157
Rotor inductance (H)	L_r	0.158
Inertia coefficient (Kg.m^2)	J	0.0056
Rated motor speed (rpm)	ω_N	1740
Rated motor frequency (Hz)	f_N	60
Rated power (kW)	P_N	3.7

D. COMPARISON BETWEEN FCS- AND CCS- MPC TECHNIQUES WITH EXPRIMENTAL RESULTS

An experimental setup has been established, as composed of 3.7 kW IM driven by a 5.6 kW two-level VSI with interface circuits. The switching devices in the inverter are IGBTs with 20 kHz switching frequency, and the dc-link voltage is 450 V. The control board is based on the 32-bit floating point TMS320F28335 DSP. Main parameters of the IM are presented in Table 1.

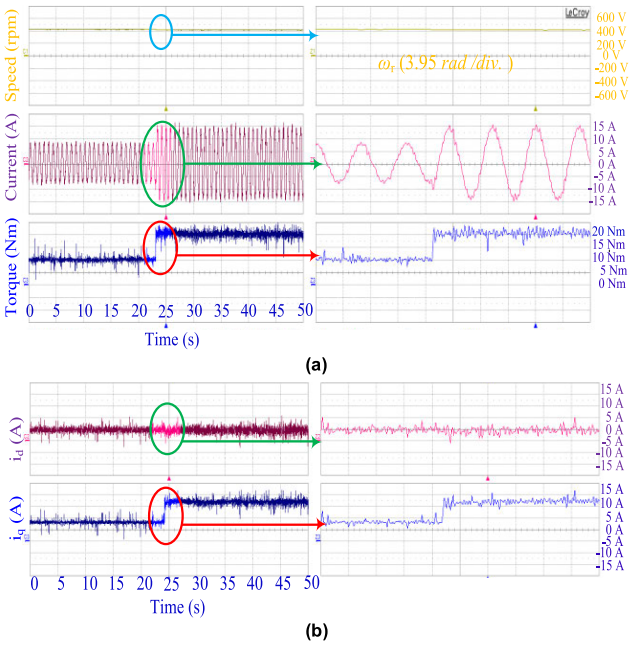

FIGURE 11. Experimental waveforms using FCS-MPC with separate duty ratio: (a) phase current and estimated torque and (b) d- and q- axis currents.

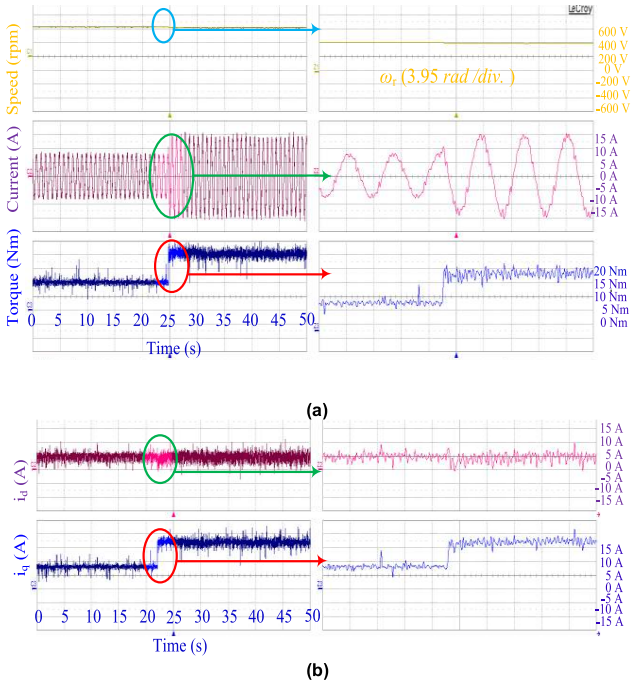

FIGURE 12. Experimental waveforms using FCS-MPC with optimization on voltage and duration simultaneously: (a) phase current and estimated torque and (b) d- and q- axis currents.

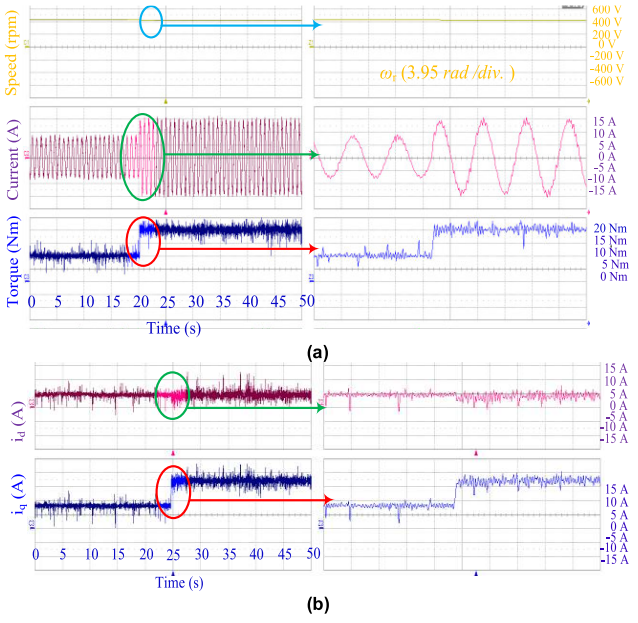

FIGURE 13. Experimental waveforms using CCS-MPC: (a) phase current and estimated torque and (b) d- and q- axis currents.

1) DYNAMIC PERFORMANCE WITH MPC FOR TORQUE CONTROL

The next experimental waveforms validate the performance of the controlled IM under the three control schemes named conventional FCS-MPC, modulated FCS-MPC, and modulated CCS-MPC, as shown in Figs. 11, 12, and 13, respectively. The three control techniques are examined for the transition from half to full rated load torque (10 to 20 Nm) and at rated speed of 1740 rpm. The speed is fixed by the second IM. The sampling frequency (10 kHz) is similar for the three algorithms. All control methods are recorded at the same DC voltage of 400 V. During this dynamic process, DC voltage, phase current, torque, and d-q currents are observed from top to bottom. It could be noticed some noise effect occurs in the waveforms because no filter is used during measuring. At the

rated speed of 1740 rpm, torque tracking is accomplished with high ripples using conventional MPC (Fig. 11), low ripples with the modulated FCS-MPC (Fig. 12)) and very low ripples with the modulated CCS-MPC (Fig. 13). It can be seen that dq-axis currents are different in the three methods, as shown in Figs 11, 12, and 13 (b). Also, from the experimental pictures, it can be observed that the modulated FCS-MPC can minimize the torque and current ripples at different torque levels, even at medium and high speeds. From close observation, it can be noticed that both the modulated FCS-MPC and CCS-MPC will deliver torque and current with less ripples than that of conventional MPC.

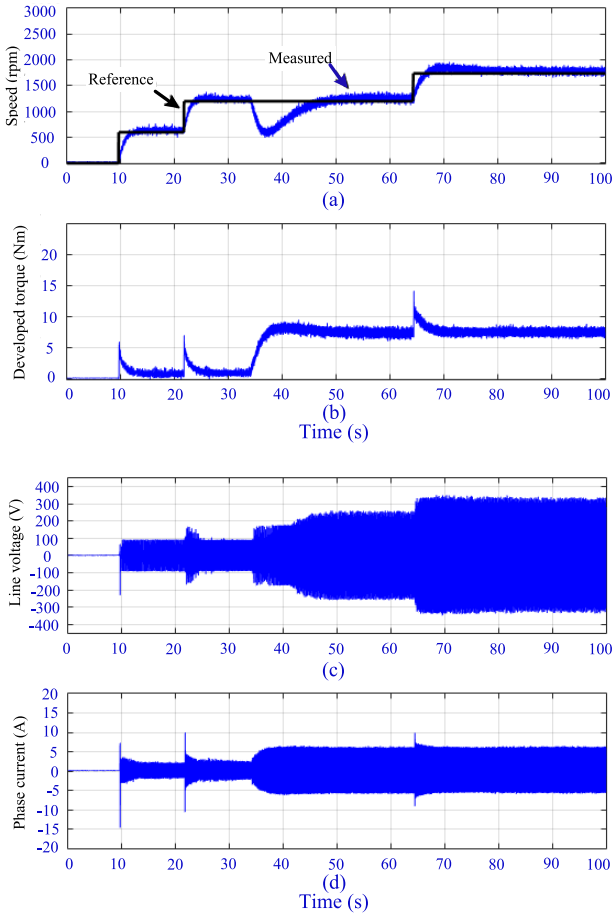

FIGURE 14. Experimental waves of FCS-MPC with separate duty cycle: (a) speed, (b) developed torque, (c) line voltage, and (d) phase current.

2) EXPERIMENTAL INVESTIGATION FOR SPEED CONTROL OF IM USING FCS- AND CCS- MPC

Experimental results for a multi upstairs operation, followed by a load impact of FCS-MPC and CCS-MPC are shown in Figs. 14 and 15, respectively. The figures depict the dynamic behavior at start up to 600 rpm, 1200 rpm, and then to rated speed of 1740 rpm. Load torque of 7.5 Nm is suddenly applied at time of 35 s. As shown in Figs. 14, 15(a), the rotor speed tracks its reference after 2 seconds, and good

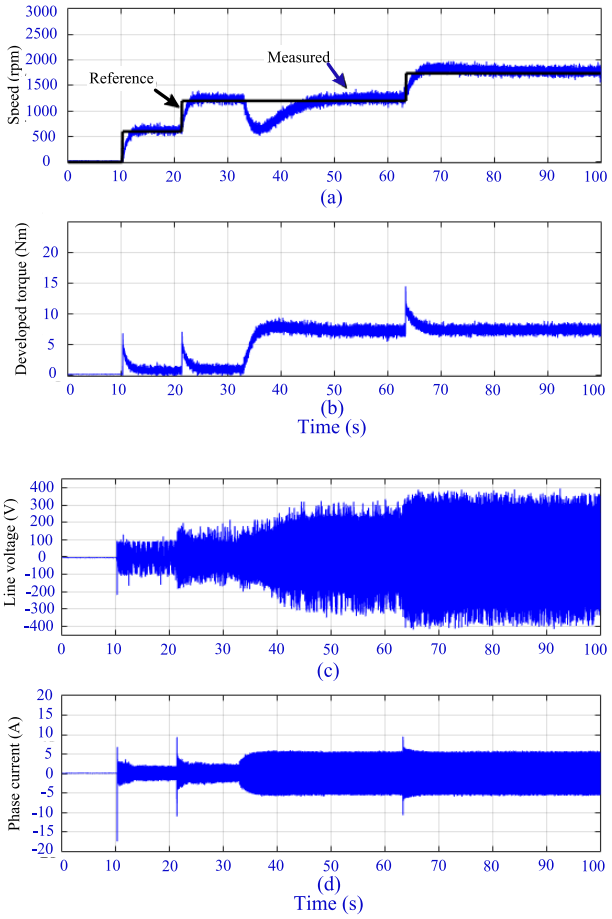

FIGURE 15. Experimental waves of CCS-MPC: (a) speed, (b) developed torque, (c) line voltage, and (d) phase current.

torque response can be observed from the waves of reference and developed torques. A successful implementation of the KF can be noticed by the effective waveforms of estimated load torque and estimated speed. At the transient time, the estimated load torque is different from the developed torque because of the inertia impact and the difference disappears at steady state. When an external load torque is suddenly applied, some delay in speed response appear. Phase current is proportional to the dynamic behavior of IM. At start-up, high current is drawn which depends on the initial flux level and the accuracy of inertia used in the model. Mechanical load torque of 7.5 Nm is suddenly added, however the phase current is gradually increased because the response of KF estimator. Also, it can be noticed that the rotor flux is increased when the load torque is increased, and the phase current components are equal to those of the maximum torque per ampere (MTPA) operation. It can be concluded, from Figs. 14 and 15 that, the performance of FCS is approximately same as that of CCS. However, the difference lies in that FCS has lower ripples in speed compared to that of CCS. The reason is that the parameters of the outer loop (integrator and KF gains) are specifically

designed for better performance for FCS, and then they are used for CCS. Therefore, torque reference, generated from the outer loop, with CCS suffering from some ripples, as shown in Figs. 14, 15(b). The line voltage of the FCS-MPC is accurately limited to 320 V, while the applied voltage of the CCS-MPC reaches a higher value. Then, the latter is mandatorily required by a constraints checker, as shown in Figs. 14, 15(c). Both methods can be controlled within the current limitations, as shown in Figs. 14, 15(d).

IV. DESIGN OF WEIGHTING FACTORS IN FCS-MPC

A. FCS-MPC WITH TUNING WEIGHTING FACTOR

Despite the previous mentioned advantages of the MPC, it is difficult to find the best value of the weighting factors, especially if the two terms have different units [70]–[77]. Furthermore, the selected weighting factor depends on the current operating point [78]. Hence, too much time and tedious offline tuning work is strongly needed if the operating point is changed. As a result, more focus from the researchers has been put forward to find the best weighting factor as one of main parts in the MPC algorithm. These methods can be classified into offline and online ones. More details are given out below.

1) OFFLINE METHODS

This method as called aggregation of functions (AOF) is based on multiplying the individual terms of the cost function by different weighting factors to balance the unit. In general, it is simple but time-consuming. In this method, extensive offline simulations are used to determine the appropriate weights based on the required object or certain criteria. Ref. [75] is considered as one of the good literatures where it introduces the guidelines to calculate the offline weighting factors in addition that the cost functions are clarified according to their values. Briefly, the calculations of the weighting factors can be selected or determined by minimizing the THD or the root-mean-square (RMS) error of the optimized parameters [79]. This method is considered as the most common in the literature for calculating the weighting factors. Moreover, an offline optimization based on the linear matrix inequality is used to obtain the weighting matrix for the state tracking error [23], [69], [80]. The main problem for this method is the need of repeating the offline simulation to get the new weighting when the operating point changes. Therefore, online methods have been usually presented to solve this kind of problem.

2) ONLINE METHODS

Different from the previous offline methods, these methods are based on the updated weighting factors for each control sample or non-weighting factors from the cost function by mathematical derivation. An optimized weighting factor for induction machine is proposed in [78], [81], where the minimum torque ripples can be obtained by calculating the weighting factor at each control sample. This proposed method has a significant impact on the torque ripple reduction, but it suffers some problems, such as high parameter dependence, complicated calculation on the weighting factor at every operating point, *etc*.

Moreover, different multi-objective optimization techniques have been used to decide the best weighting factor, such as Ranked method, Fuzzy decision algorithm, VlseKriterijuska Optimizacija I Komoromisno Resenje (VIKOR) method [31], and so on. In [73], one ranked method is used to select the best switching vector among all the switching vectors after storing the evaluation of the cost function for both torque and flux. Based on this ranked method, the weighting factor can be omitted. In the same way, the fuzzy decision method can be used to select the best voltage vector based on the membership function concept [77], [79]. In this method, an individual cost function together with the fuzzy decision can evaluate effectively. Moreover, a new technique is developed for the PTC of IM drive depending on the VIKOR method [82], which is suitable to solve optimization problems with inconsistent objective functions for its strong ability to deal with multi-criteria cases. In addition, it can also give one index to each switching vector, in which the minimum one can be selected as the best candidate.

Furthermore, one linear matrix inequality (LMI) optimization technique has been used to find out the best value of the weighting factors that achieve the condition of stability [20]. In order to reduce the on-line computational effort, a set of weighting-matrix values are obtained off-line depending on the regions of operational speed.

Finally, different techniques for the weighting factor selections are summarized in Fig. 16. It is seen that the dark shadow represents the online methods and the yellow shadow the offline methods.

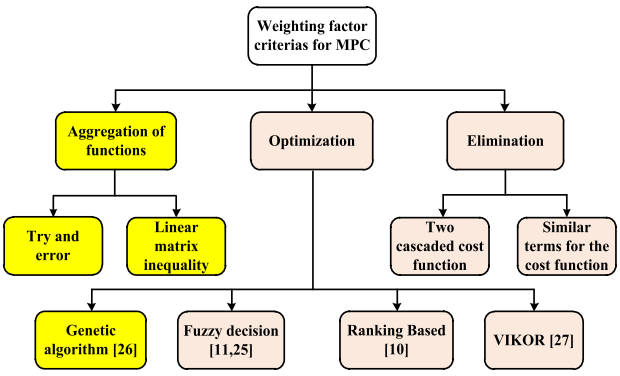

FIGURE 16. Different weighting factor criteria for the MPC.

B. FCS-MPC WITHOUT WEIGHTING FACTOR

In general, the conventional cost function of the FS-MPDTC consists of the absolute torque and stator flux-linkage errors. Therefore, it needs a weighting factor to balance the unit of the two terms, which gives one priority to one of them if suitable [83]. Recently, great efforts from the researchers have been done to overcome the problems adding weighting

factors to the cost function, as mentioned in [34], [36], [73], [84]–[91]. These works of eliminating weighting factors are typically classified into two parts, as illustrated in Fig. 16. More details will be introduced as follows.

1) SIMILAR ITEMS IN THE COST FUNCTIONS FOR ELIMINATING THE WEIGHTING FACTOR

In [34], there are two techniques of weighting factor less are proposed. The cost function of the first technique is similar to that of the conventional FCS-MPDTC, but it is based on a variable weighting factor. In brief, this factor is related to the flux ripple where it can be considered as a hard constraint without a complex tuning process. The cost function and the constraint limits based on these techniques are given by

$$g = \left|T_e^* - T_e\left(k+1\right)\right| + K_\psi \left|\psi_s^* - \psi_s\left(k+1\right)\right| \quad (14)$$

$$K_\psi = \begin{cases} \infty, & \text{if } \left\|\psi_s^* - \left\|\psi_s^*\right\|_{(k+1)}\right\| > \psi_{ripple} \\ 0, & \text{otherwise} \end{cases} \quad (15)$$

It is the first method for eliminating weighting factor (EWF), as simplified by EWF-MPDTC-I. Meanwhile, the second technique for EWF is based on replacing the flux by one term with the same unit as the thrust (EWF-MPDTC-II). Hence, in this way, the weighting factor can be omitted. Also, the main idea of the second technique is presented for the PMSM based wind power system, where the cost function includes both torque and reactive torque errors [91]. The new cost function of such control technique is given by

$$g = \left|T_{eref} - T_e\left(k+1\right)\right| + \left|T_{evref} - T_{ev}\left(k+1\right)\right| \quad (16)$$

where

$$T_{ev}\left(k+1\right) = \frac{3}{2} n_p \begin{pmatrix} \psi_{s\alpha}\left(k+1\right) i_{s\alpha}\left(k+1\right) \\ +\psi_{s\beta}\left(k+1\right) i_{s\beta}\left(k+1\right) \end{pmatrix} \quad (17)$$

The previous two techniques of weighting less method suffer from some demerits, such as great computation time in the prediction step, where the torque and the stator current should be predicted. Also, the dependence upon the machine parameters for the stator current and the torque prediction would result in high errors in the prediction stage. Therefore, other control methods have been presented to overcome these demerits associated with the previous weighting less factor, and hence decreasing the calculation time greatly. These control methods can eliminate the weighting factor mostly based on one cost function. Therefore, the relationship between torque and stator flux is studied to eliminate the weighting factor. By full mathematical analysis, only the stator flux can be employed in the cost function, as called model predictive direct flux control (MPDFC). Till now, such method has been widely studied by many experts [36], [84], [92], [93]. The cost function for this method is given by

$$g = \left|\psi_{\alpha s}^* - \psi_{\alpha s}\left(k+1\right)\right| + \left|\psi_{\beta s}^* - \psi_{\beta s}\left(k+1\right)\right| \quad (18)$$

In the method as proposed in [84], [88] the reference stator flux vector value is equivalently calculated from the stator flux magnitude and the reference torque value in MPTC based on the model of IM. As only the tracking error of the stator flux vector is evaluated in the cost function, the weighting factor can be eliminated effectively. Moreover, the control complexity can be significantly reduced in comparison to the conventional MPTC, because the complicated prediction of stator current is no longer required [94].

Meanwhile, some improvements have been made to the aforementioned methods [86], [95], where the predictions of the control parameters are calculated based on one predefined switching table. Due to the significant computational burden, the table output is based on the torque error and the stator flux location, so as to give some delay compensations to the implementation process. The block diagram is illustrated in Fig. 17.

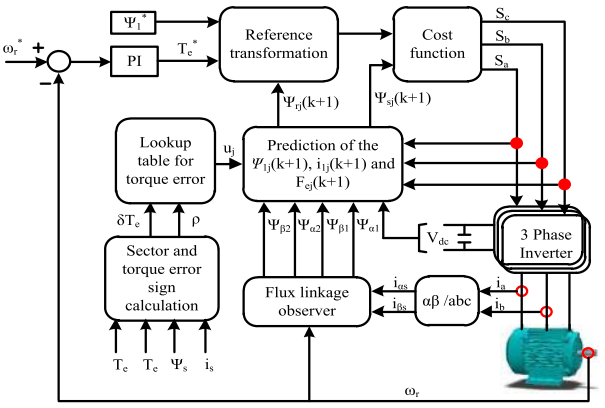

FIGURE 17. Block diagram of the simplified FCS-MPDTC without weighting factor for the IM.

Furthermore, a novel MPTC with a fast response is proposed in [36] for PMSM drives, where the reference torque is converted to reference stator flux-linkage in d-axis and q-axis, totally different from those in α-axis and β-axis as presented in [84], [92]. Besides, Pontryagin's Maximum Principle is applied during the transient process to get much faster dynamic response. It can be used for designing the minimum time flux linkage trajectories from the initial state to the reference state. Another control method without weighting factor is presented in [93], where the angle of the flux is obtained by another way, also different from the method as presented in [84], [92]. The block diagram of this control method is illustrated in Fig. 18. It is presented for LIMs, where the error between the reference thrust and the actual value thrust can be obtained by

$$\Delta F_e = F_e^* - F_e = \frac{3}{2}\frac{\pi}{\tau}\frac{1}{\tau_l \sigma}\left|\lambda_1\right|\left|\lambda_2\right|\left(\sin\left(\theta_{12} + \delta_{\lambda 1}\right) - \sin\left(\theta_{12}\right)\right) \quad (19)$$

Although this method eliminates the weighting factor, a PI controller has been added which needs some tuning work for the gains.

Comparison between different MPC techniques is presented. These techniques manly include weighting factor

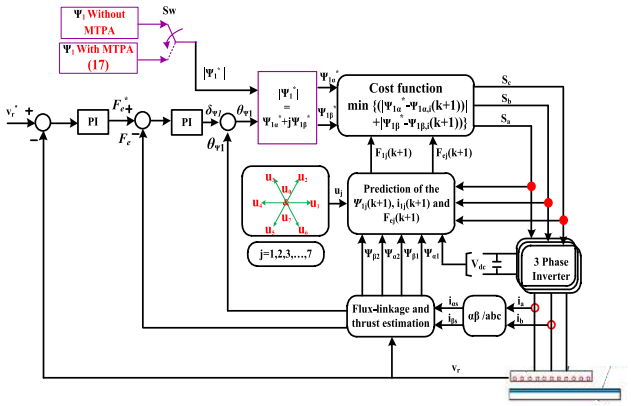

FIGURE 18. The proposed MTPA based the FCS-MPDFC for the LIM drive system [93].

model predictive direct thrust control (WF-MPDTC), EWF-MPDTC-I, EWF-MPDTC-II, MPDFC [92], and fuzzy decision based MPDTC (F-MPDTC) [77]. These five different MPDTC techniques are tested under similar thrust load (100 N) and flux linkage (0.5 Wb). The values of the thrust and flux tracking performance are fully examined at different levels of linear speed changing from 1 to 10 m/s. Furthermore, the thrust and flux ripples are calculated under the same condition. Related results are shown in Fig.19 (a)-(d), respectively. As seen from these pictures, it is noticed that the thrust and flux tracking errors for all methods would increase with the rising speed. Meanwhile, both flux and thrust ripples of F-MPDTC and MPDFC are higher than those of EWF-MPDTC-I and EWF-MPDTC-II, although the process of tuning weighting factor is eliminated. Moreover, Table 2 concludes some features of the five control methods, including dynamic response, switching frequency, thrust and flux ripples.

TABLE 2. Comparison between the five control methods [34].

Item	Dynamic Response	Switching frequency	Ripples
WF-MPDTC	Fast	Medium	Medium thrust ripples, but low flux ripples
EWF-MPDTC-I	Fast	Medium	Low
EWF-MPDTC-II	Fast	Medium	Medium flux ripples, but low thrust ripples
MPDFC	Fast	Low	High
F-MPDTC	Fast	Low	High

Another control method is proposed in [87] where the weighting factor is eliminated and the cost function is based on the voltage vector rather than the flux-linkage. It uses the output voltage in the designed cost function where the deadbeat is employed to calculate the reference voltage vector. However, all available voltage vectors should be examined in the design process of cost function. For the use of the deadbeat control with the predictive direct voltage control, the robustness capability is becoming a little weaker, which

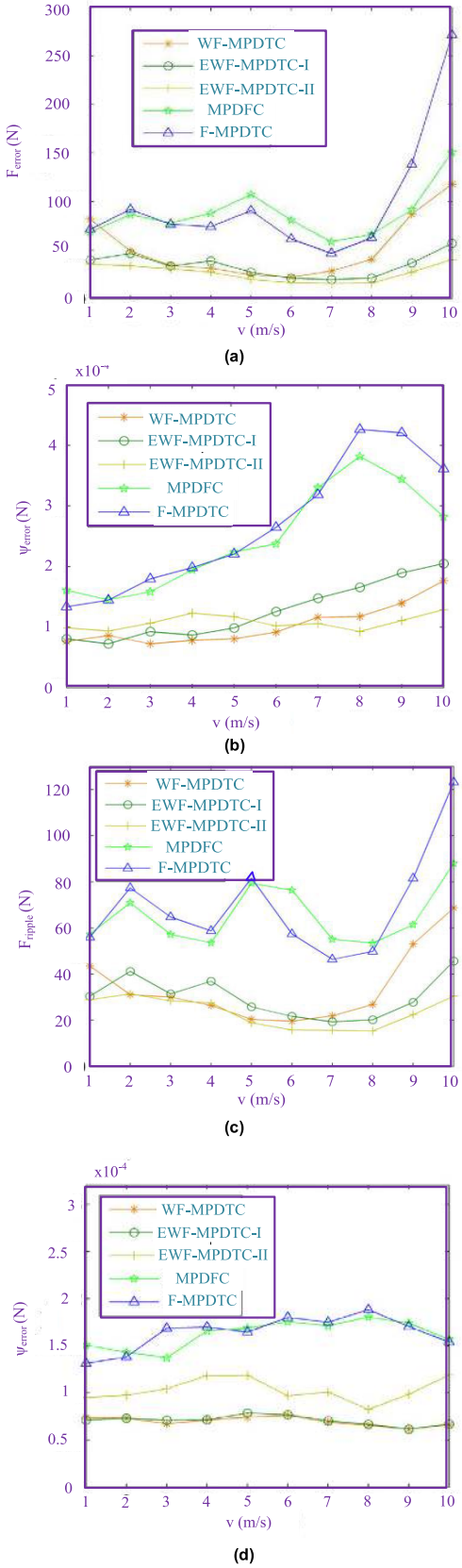

FIGURE 19. Comparative performance of different MPTC methods under the same switching frequency: (a) thrust tracking errors, (b) flux tracking errors, (c) thrust ripples, and (d) flux ripples [34].

mainly comes from the influence by calculating the similar voltage references. Hence, an MRAS Luenberger observer is used to improve the robustness of the proposed method. Moreover, a new technique for gain design is presented to improve the robustness and stability of the overall control system. In this way, although the robustness of the control system is strengthened, the calculation burden is heavily increased.

2) CASCADED COST FUNCTIONS WITH SIMILAR ITEMS FOR ELIMINATING THE WEIGHTING FACTOR

Also, a new idea of weighting less has been presented in other literature works with different names, such as parallel predictive torque control, dynamic cost function, multi objective ranking, variable cost functions' sequence design [73], [85], [89], [90], and so on. In [85], one solution for weighting less factor has been presented, as called one parallel predictive torque control (PPTC). This method has predefined constraints that can simultaneously optimize both flux and torque terms. Moreover, the switching states are selected in an adaptive mechanism. As mentioned before, the implementation process of this control method is based on the parallel structure to optimize both torque and flux cost functions, which is different from other cost functions with one fixed weighting factor or multiple control objectives. While a little difference in this algorithm, main control objectives can be achieved simultaneously but independently. This method can be improved by using boundaries for both torque and flux tracking errors. Finally, one adaptive selection mechanism is used to evaluate the voltage vectors, which can make both flux and torque magnitude errors within the predefined boundaries. Full comparison between the conventional PTC and the PPTC is illustrated in Table 3. But in [90], one novel dynamic cost function is presented to eliminate the usage of weighting factor from the cost function. In general, the cost function is based on two dynamic per-unit values where the errors for both stator flux and torque are converted to dynamic per-unit values with the same order of magnitude. More details can be summarized as follows.

TABLE 3. Comparison between PTC and PPTC.

Item	PTC	PPTC
Calculation efforts	Low	Low
Stator current THD	Medium	Medium
Sensitivity to Rs	Higher	Lower
Switching frequency	Higher	Lower
Flux ripple	Higher	Lower
Torque mean squared error	Higher	Lower
PWM block	No	No
Sensitivity to Rr	Low	Low
Dynamic response	Fast	Fast

The dynamic cost function is defined by

$$G_{0i} = G_{1i} + G_{2i} \tag{20}$$

where

$$G_{1i} = \frac{g_{1i} - g_{1\min}}{g_{1\max} - g_{1\min}} \tag{21}$$

$$G_{2i} = \frac{g_{2i} - g_{2\min}}{g_{2max} - g_{2\min}} \tag{22}$$

where g_{1i} is the torque error at every voltage vector, g_{1max} the maximum value of g_{1i}, and g_{1min} the minimum value of g_{1i}. Meanwhile, g_{2i} is the stator flux error at every voltage vector, g_{2max} the maximum value of g_{2i}, and g_{2min} the minimum value of g_{2i}. It can be observed from (21) and (22), that both torque error and flux linkage error are converted to one dynamic per-unit value. The range of variations to both G_{1i} and G_{2i} are changed from 0 to 1. In order to minimize the torque and stator flux-linkage errors, the values of G_{1i} and G_{2i} should be minimized as much as possible. Therefore, a new cost function is proposed in (20), as called one dynamic cost function, which is varying dynamically per control period. Mostly, the cost function does not require a weighting factor because both G_{1i} and G_{2i} have the same order of magnitude. It is found that the main problem for cost function is the high computation burden.

Furthermore, one new predictive control method has been proposed in [73] which is based on ranking approach for multi-objective optimization instead of single cost function. The main advantage of this ranking approach is unnecessary to tune the weighting factors. In this method, two cost functions are used (i.e. one for the torque error, and the other for stator flux-linkage error). These two different cost functions are given out by

$$g_1 = \left| T_e^* - T_e^{k+2}\left(V_s^{k+1}\right) \right| \tag{23}$$

$$g_2 = \left| \left\| \psi_s^* \right\| - \left\| \psi_s^{k+2}\left(V_s^{k+1}\right) \right\| \right| \tag{24}$$

where g_1 and g_2 are the torque and stator flux the errors, respectively.

The multi-objective ranking-based technique can evaluate the values of the two cost functions for each possible voltage vector, separately. The first step is storing the values for g_1 and g_2 resulted from the evaluation of each voltage vector. After that, a ranking value to each error value is assigned, where the voltage vectors with higher error are assigned a higher ranking, while the others a lower ranking. These processes can be illustrated by

$$g_1\left(V_s^{k+1}\right) \rightarrow r_1\left(V_s^{k+1}\right) \tag{25}$$

$$g_2\left(V_s^{k+1}\right) \rightarrow r_2\left(V_s^{k+1}\right) \tag{26}$$

where $r_1(\mathrm{V_s^{k+1}})$ and $r_2(\mathrm{V_s^{k+1}})$ are the ranking values for g_1 and g_2, respectively. Based on these ranking values, the relative quality of each voltage vector is determined with respect to the remaining voltage vectors. These ranking values are unit less, but their corresponding error values have units, such as newton meter, weber, *etc*. From the point of torque error, the best voltage vector can be decided by the lowest ranking value. Also, from the point of stator flux-linkage

error, in the same way, the optimum voltage vector can be selected. In order to determine the best one among the overall switching vectors, one average criterion is employed in this work, as given out by

$$V_{opt} = \min_{\{V_0,\ldots,V_7\}} \frac{r_1\left(V_s^{k+1}\right) + r_2\left(V_s^{k+1}\right)}{2} \tag{27}$$

In the genetic algorithms, this evolutionary optimization algorithms are commonly used [96], [97]. Furthermore, another idea has been presented in [89] to eliminate the use of weighting factor. It is based on the cascaded cost functions optimization for both torque and flux linkage. Main working principles can be summarized as follows.

Firstly, two cost functions are proposed, as given out by

$$g_T = \left|T_e\left(k+2\right) - T_e^*\right| \tag{28}$$

$$g_\psi = \left|i_d(k+2) - 0\right| \tag{29}$$

where g_T and g_ψ are the cost functions for torque and flux linkage, respectively. Secondly, based on the priority of the control target, one of these two cost functions is evaluated by all of the switching voltage vectors. Thirdly, the best three voltage vectors are then given to the second cost function. Finally, the voltage vector that minimizes the second cost function is selected as the globally optimized one and its switching states are sent to the inverter directly.

V. FCS-MPDTC WITH MAXIMUM TORQUE PER AMPERE

This section discusses different method of maximum torque per ampere (MTPA) for RIMs and MTPA for LIMs. The adoption of MTPA leads to lower input current, lower losses, and hence higher efficiency. In order to enhance the performance of the drive system based on the FS-MPC, some criteria have been added to the cost function, such as MTPA, current limitation, and so on [21], [60], [98]–[100]. In [101] and [102], the criteria of MTPA is adopted to increase the efficiency, and state limitation for maximizing their admissible values. Moreover, another criterion is added in the cost function to limit the voltage [99], which can strengthen the field weakening ability, more attractive to the high speed operation. The final cost function of the proposed methods in [21], [99], [101] is given out by

$$C(k) = \sum_{i=0}^{N} \left(\lambda_T c_T\left(k+1\right) + \lambda_A c_A\left(k+1\right) + \lambda_L c_L\left(k+1\right)\right) \tag{30}$$

where $C_T(k+1)$, $C_A(k+1)$, and $C_L\ (k+1)$ are the terms which are responsible for minimizing the torque error, MTPA criteria, and current limitation, respectively. Meanwhile, λ_T, λ_A, and λ_L are the weighting factors, which clarify the importance of very term in the group. More details about the equations and values of these terms can be found in the references [21], [99], [101]. In the similar way, the MTPA is presented in [60] but with an improvement to the speed control law, where a quasi-time-optimal is used instead of the PI controller. All these control methods mentioned above are presented for the PMSM successfully.

On the other hand, for RIMs, a new MTPA based on the FS-MPC is presented in [100]. This control method is contrary to the previous control method where the cost function includes the torque error and the angle error. The angle error is calculated from the difference between the angle of predicted stator current and the angle of the predicted rotor flux in one side and $\pi/4$ on the other side. Therefore, this control method is also called finite-set model predictive direct angle control (FS-MPDAC). The advantages of this control method are the capability of achieving the MTPA with only one weighting factor rather than four weighting factors. Meanwhile, the cost function in the previous control methods consists of the torque error and the stator flux-linkage error, which needs four weighting factors to achieve the MTPA.

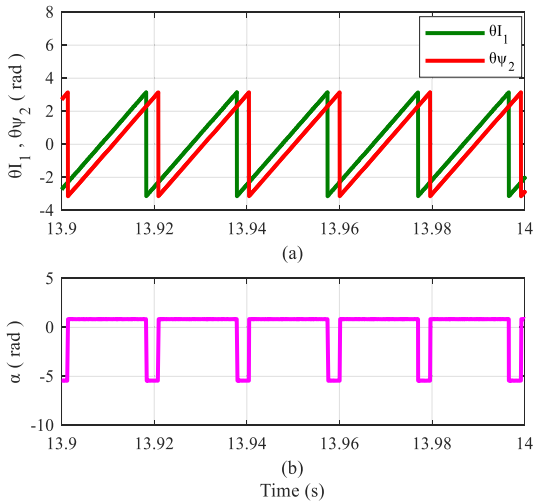

FIGURE 20. Angle and angle difference between current and flux: (a) angle and (b) angle difference.

Meanwhile, as to the LIMs, there are some control methods as proposed to get the MTPA, some of which are based on the FS-MPC methods. Here, the authors mainly focus on the MTPA based FCS-MPC as proposed in couple of papers [51], [93], [98], [100]. The presented control method in [100] has been improved and applied for LIMs in [98]. The MTPA method in [98] is based on the cost function, in which the second term includes the *cosine* angle error $|\cos(\alpha(k+1)) - \cos(\pi/4))|$ instead of the direct angle error as illustrated in [100]. The advantages of using the cosine difference are: (1) The direct difference between the two angles contains periodic changes as shown in Fig. 20. Meanwhile, no periodic change is generated by using cosine difference as shown in Fig. 21. (2) According to the derivation of the second derivative of thrust, the d-axis current must be positive while the q-axis current may be positive or negative. (3) The cosine function is positive in the first and fourth quadrants, which can match the acceleration and deceleration working processes. The block

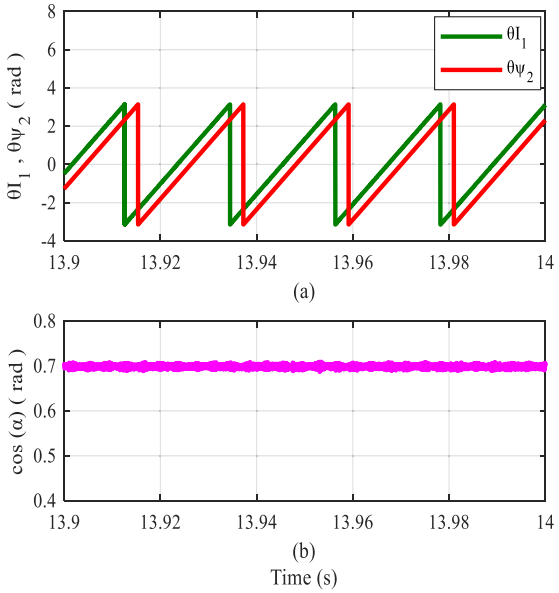

FIGURE 21. Angle and cosine difference between current and flux: (a) angle and (b) cosine difference [98].

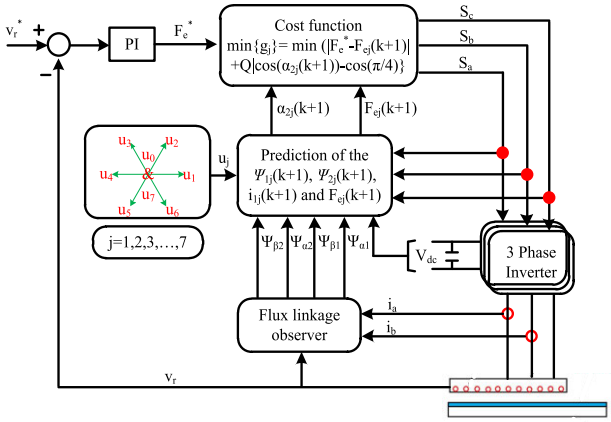

FIGURE 22. Block diagram of the MTPA based the FS-MPDAC for the LIM drive system [98].

diagram of this control method is illustrated in Fig. 22. The computation time for FS-MPDAC and the FS-MPDTC are shown in Fig 23 (a) and (b), respectively.

However, the primary flux-linkage error is not included in the cost function of FS-MPDAC, which results in rising ripples of the primary flux-linkage, more calculation time in the prediction stage. Even worse, the machine would not start to work for the absence of enough flux linkage. Consequently, one FS-MPDTC with MTPA is proposed in [51] to overcome these shortcomings, where the primary flux-linkage is calculated based on the MTPA condition, and inserted in the FS-MPDTC with only one weighting factor to reduce the copper loss.

Furthermore, a limitation of the primary current is inserted in the cost function to prevent the machine from over current. Also, the parameter sensitivity analysis of the optimal flux calculation is studied to check the impact of the errors on

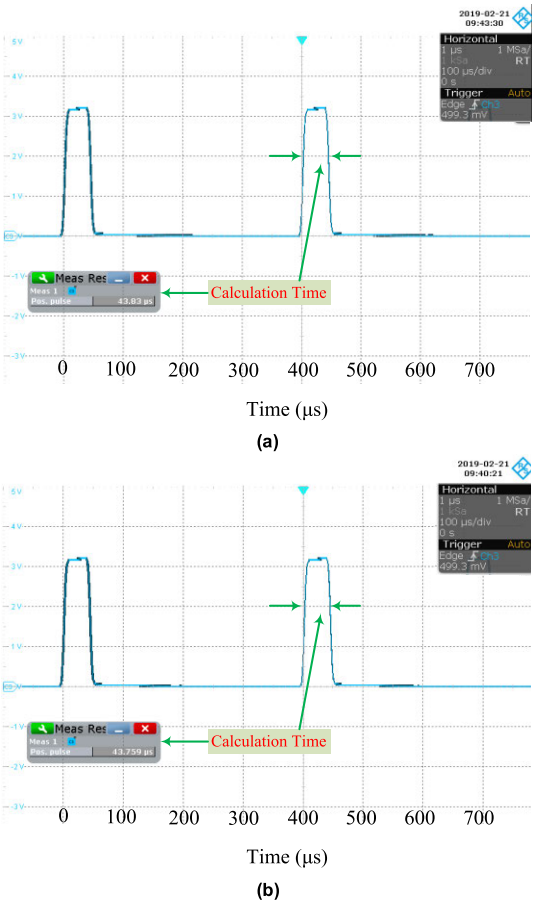

FIGURE 23. Comparison of computation time: (a) Computation time for FS-MPDAC and (b) Computation time for FS-MPDTC.

the accuracy of the proposed control strategy. The proposed FCS-MPDTCs with and without MTPA are tested for the LIM drive system, in which main parameters are listed in Appendix Section. In this case, the method is verified under the thrust load of 50 N, linear speed of 7.5 m/s and sample time of 2×10^{-4}s. Firstly, one arc induction machine (AIM) with large radius, as one demonstrator for the practical LIM, is controlled by the FS-MPDTC without MTPA for approximate 20 s, then the MTPA is activated. The primary voltage is kept constant for the FCS-MPDTC methods with and without MTPA. It is known that the control method with MTPA is successful in regulating the linear speed at 7.5 m/s, as illustrated in Fig. 24 (a). The primary flux is regulated around the reference value, as shown in Fig. 24 (b). Meanwhile, Fig. 24 (c) shows the phase-A primary current, which demonstrates that the current is decreased by 20% when the MTPA is switched on. Furthermore, the electromagnetic thrust is maintained constant at the required load 50 N with small ripples at the switching on of MTPA, as shown in Fig. 24 (d).

The main problem of this control method is the great dependence on the weighting factor. Briefly, it can be solved by using the weighting less MPC, as discussed in the previous section.

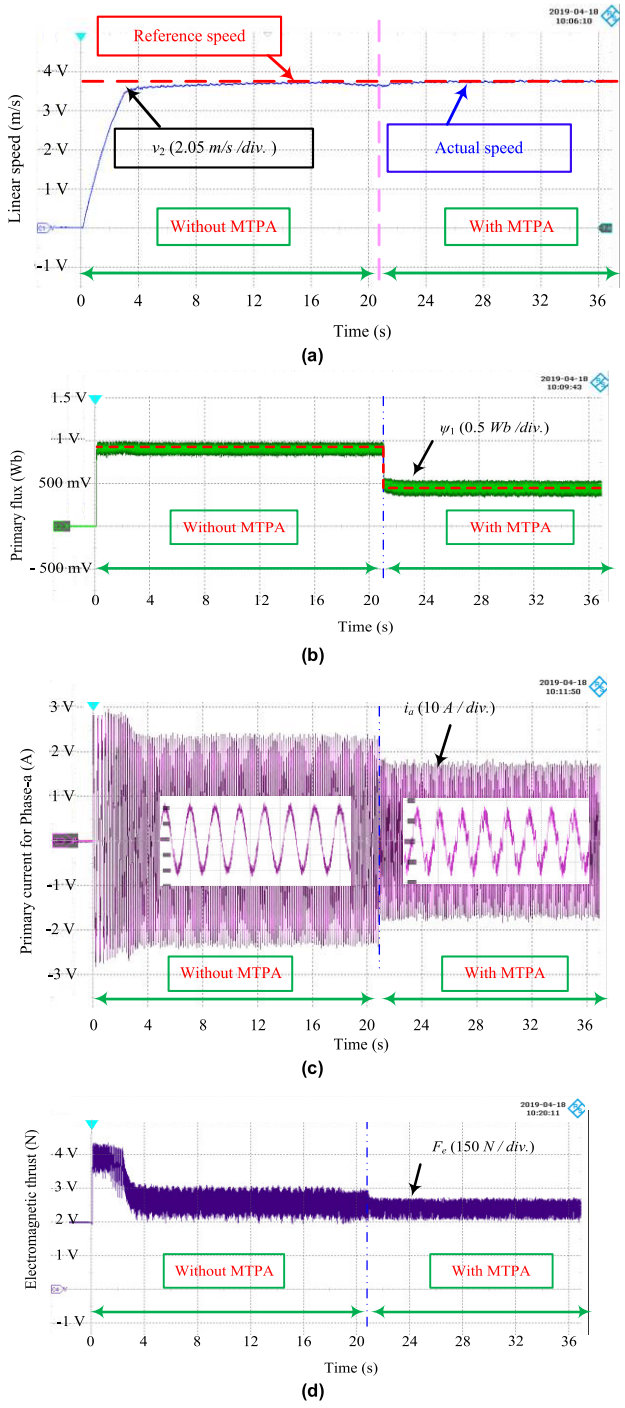

FIGURE 24. Experimental validation of the FCS-MPDTC methods with and without MTPA: (a) linear speed, (b) primary flux-linkage, (c) primary phase-A current, and (d) thrust [51].

VI. MODEL PREDICTIVE DIRECT SPEED CONTROL

A. PI-MPCC CASCADED FOR AC DRIVES

In this case, one PI speed control is used for tracking the speed command without estimation on the load torque. However, the drive performance could not be guaranteed very excellent at different operating conditions.

B. MPSC-MPCC CASCADED FOR AC DRIVES

By literature survey, just a few works on direct speed control based on MPC (DSC-MPC) control systems have been proposed for both PMSM and IM drives. In [103], the reference speed of one LIM is effectively tracked by the MPC control without any PI controllers. Recently, a cascaded predictive control approach has been proposed to regulate the stator current and the speed of electrical machine individually via two separate cost functions, [104]–[107]. In [106], two cost functions with different weighting matrices are used to design the MPC method that greatly increases the computational burden and worsens the current ripples. The strategy of [107] has used a mechanical dynamic model to determine a reference torque that can get excellent tracking for the reference speed, in which the cost function only controls the stator currents.

Moreover, it is also possible to avoid the cascaded structure using a single controller for all variables, including speed, flux, current, and so on. A cascade-free predictive control approach has been presented for the PMSM [101], [108] and IM [109], which can regulate both the stator current and the speed via one single cost function. Both simulation and experiments have demonstrated that, this method can get satisfactory results, while it suffers a little complexity, because the cost function includes many factors to be determined heuristically.

Till now, different kinds of direct speed predictive control methods have been investigated in [4], [110]–[113]. In these investigations, a new control method based on the FCS-MPC is presented for direct speed control of RMs without any linear controllers. In [112], an output feedback discrete-time MPC algorithm is used to achieve a robust predictive speed regulation for a generic dc-dc converter-driven permanent magnet direct current motors (PMDCMs). This motor requires high-precision speed regulation in industry, which is facing with big challenges due to parametric uncertainties, time varying load torque disturbances, exogenous nonlinear traits of converter, *etc*. Therefore, a new discrete-time reduced-order generalized proportional-integral observer (GPIO) is presented, which can effectively reconstruct the lumped disturbances and the virtual system states. The output speed prediction can be obtained from the calculation of the GPIO estimated values.

On the other hand, for three-phase AC machines, the weighting less MPC with reducing computation burden is still considered big challenges for the conventional speed prediction control. In order to solve such problem, one model-predictive direct-speed control (MP-DSC) method based on direct voltage-vector selection is proposed in [4]. In this method, the deadbeat control principle is used to obtain the reference voltage vector, and hence only reference voltage vector is employed in the cost function. Thus, the weighting factor can be eliminated, and then only the error between the reference voltage vector and the candidate voltage vector is included in the cost function. Besides, the load torque and the motor speed are estimated by using an extended sliding-mode

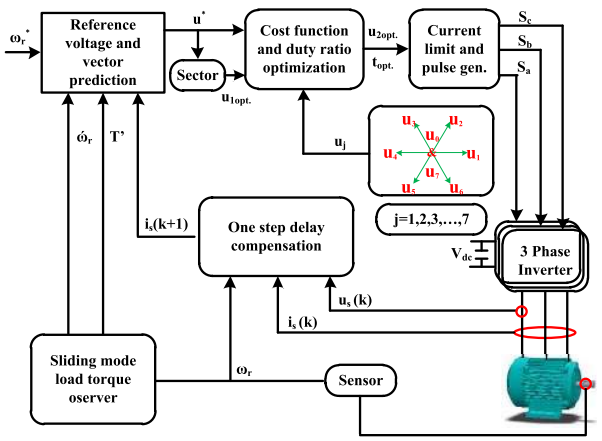

FIGURE 25. Control diagram of the MP-DSC method.

load–torque observer, which can enhance the 5system robustness and decrease the measurement noise effectively. The block diagram of this control method is illustrated in Fig. 25.

C. CASCADED-FREE MPDSC FOR AC DRIVES

For the same objective of eliminating the cascaded loop structure while in different way, a new direct predictive speed control (DPSC) method for PMSMs is developed in [111], where two cost functions are presented. The general block diagram is shown in Fig. 26.

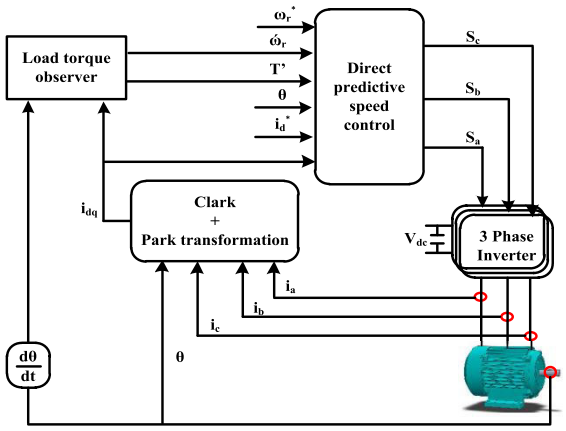

FIGURE 26. Block scheme of the DPSC method [111].

The first cost function includes a novel sliding manifold term to realize the speed/current tracking, which is simple enough to be easily implemented, as given by

$$g = |S| + \lambda_d \left(i_d\left(k+1\right)\right)^2 + \lambda_m \left(\omega_m^* - \omega_m\left(k+1\right)\right)^2 + F_C \tag{31}$$

where S is the sliding manifold, $i_d d$-axis current, $\left(\omega_m^* - \omega_m\left(k+1\right)\right)^2$ the speed error. Meanwhile, λ_d, λ_m are weighting factors.

The second cost function consists of three terms as described by

$$g = |F_{ss}| + \lambda_{st}\delta\left(\Delta\omega_m\right)F_{st} + F_C \tag{32}$$

where F_{ss} is the steady-state term, F_{st} the transient term, F_C the constraint-related term, and λ_{st} the weighting factor. Mostly, λ_{st} represents a trade-off between the fast dynamic response and good steady-state performance.

The constraint-related term is

$$g = |F_{ss}| + \lambda_{st}\delta\left(\Delta\omega_m\right)F_{st} + F_C \tag{33}$$

The advantages of this control structure include its dynamically adjustable weighting factors and no need for long prediction horizons. Detailed comparisons between PI-MPCC, DPSC 1, and DPSC 2, are made under the rated speed with no load and loading conditions, as listed in Tables 4 and 5, respectively.

TABLE 4. Comparison between PI-PCC, DPSC 1, and DPSC 2 at no load.

Item	PI-PCC	DPSC 1	DPSC 2
Speed ripple (rad/s)	1.21	0.98	0.97
Settling time (s)	92	73	78
Sum of abs. error (rad/s)	2933.8	2134.3	2164.0
Current ripple in id/iq (A)	6.13/6.76	6.78/8.67	7.22/9.50
Sum of speed error (rad/s)	-88.16	33.31	30.89

TABLE 5. Comparison between PI-PCC, DPSC 1, and DPSC 2 at loading.

Item	PI-PCC	DPSC 1	DPSC 2
Speed ripple (rad/s)	1.00	0.69	0.87
Settling time (s)	923/1052	78/72	81/74
Sum of abs. error (rad/s)	1074.8	792.24	1127.5
Current ripple in id/iq (A)	5.86/7.32	6.95/6.80	6.88/8.02
Peak (rad/s)	164.58	159.29	158.91
Sum of speed error (rad/s)	-332.84	-6.07	-551.05

Also in [113], the model predictive direct speed control (MPDSC) is proposed for servo drives to achieve high dynamics and reliability on the speed control. This control structure can eliminate the cascaded PI controller by predicting the future speed in discrete steps. Then, the speed and flux tracking criterion is evaluated to select the optimal voltage vector for the motor control. For improving the system reliability and reducing the system cost, an observer for load torque is used to estimate the actual load torque. Furthermore, the cost function is incorporated by a torque suppression factor in order to avoid overshoots during rapid speed variation and torque oscillations. Moreover, both dynamic and the steady-state drive performance have been enhanced by a myopic prediction correction method, as validated by comprehensive simulation and hardware-in-the-loop analysis.

Furthermore, the cascaded-free MPC for the speed control of IMs has been proposed in [109] by using a single optimization algorithm. This type cascaded-free MPC is presented for FCS-MPC which suffers from high current and torque ripples. Meanwhile, the CCS-MPC can get the optimum control voltage via combination of a single optimization algorithm with the nature of continuous control set. The synergy

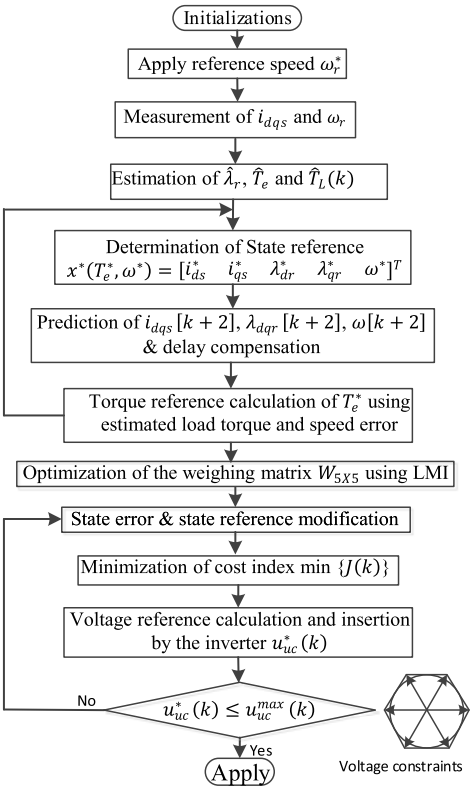

FIGURE 27. Flowchart of employing CCS-MPC controller for direct speed control of AC drive system.

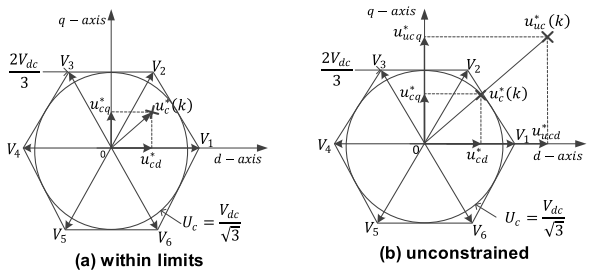

FIGURE 28. Six input voltage vectors [54].

resulting from this combination of two leading benefits can diversify and broaden CCS-MPC methods to industry. The Flowchart of CCS-MPC controller for the direct speed control of ac drives is illustrated in Fig. 27.

VII. STABILITY OF MPC

As mentioned before the CCS-MPC is based on the calculation of the voltage vectors and then applying the PWM technique. Therefore, the performance of the system under the optimal selected voltage vector has to be evaluated to ensure its stability. In case of the optimizer voltage $u_c^*(k)$ of the optimization problem is the same as the unconstraint $u_{uc}^*(k)$ as shown in Fig. R9 (a) (Fig. 28 (a) in the revised manuscript), it will be within limit i.e. $\left\|u_{uc}^*(k)\right\| \le V_{s\max}$. On the other hand, if $\left\|u_{uc}^*(k)\right\| \ge V_{s\max}$, the feasible set

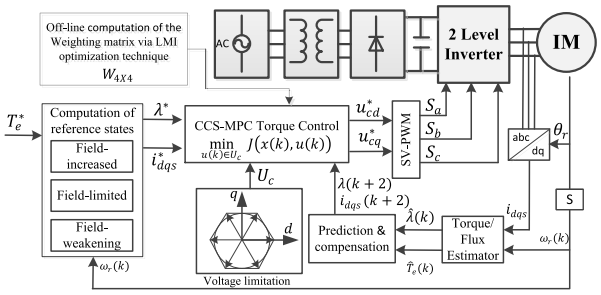

FIGURE 29. The configuration of the CCS-MPC torque control of IM [54].

of inputs satisfying can be represented as a circle in the dq-axis coordinates as given in Fig. R9 (b) (Fig. 28 (b) in the revised manuscript). In this case it is clear that $u_c^*(k)$ is at the tangential point of the boundary of the circle with the level set of the index function $J(k)$. Consequently, the selected set point of $u_c^*(k)$ is determined by finding the intersection point of the boundary of the feasible input region with the line segment from the point $u_c^*(k) = 0$ to $u_{uc}^*(k)$. Therefore, the MPC algorithm for the $u_c^*(k)$ is established by

$$u_c^*(k) = \begin{cases} u_{uc}^*(k) & \text{if } \left\|u_{uc}^*(k)\right\| \le V_{s\max} \\ \dfrac{V_{s\max}}{\left\|u_c^*(k)\right\|} u_{uc}^*(k) & \text{if } \left\|u_{uc}^*(k)\right\| \ge V_{s\max} \end{cases} \tag{34}$$

To guarantee and insure the closed loop stability of the MPC, the torque reference T_e^* and its reference state x^* are assumed constants. The steady-state input u^* can be considered to satisfy

$$x^* = Ax^* + Bu^* \tag{35}$$

It can be assumed that steady-state input u^* is belonging to the appropriate region shown in Fig. R10 (Fig. 29 in the revised manuscript). Based on the compensation delay and with $u[k] = u^*$, the state propagation can be given by

$$x[k+2] = Ax[k+1] + Bu[k] \tag{36}$$

The following relation can be get by subtracting (36) from (35)

$$e[k+2] = Ae[k+1] \tag{37}$$

where $e[k] = x^* - x^*[k]$ is the error difference. With the help of (37), the cost index difference is

$$\begin{aligned} &J(k) - J(k-1) \\ &\quad = e^T[k+2]We[k+2] - e^T[k+1]We[k+1] \\ &\quad = e^T[k]\left(A^T WA - W\right)e[k] \end{aligned} \tag{38}$$

From (38), the condition of $W - A^T WA > 0$ can guarantee

$$\Delta J(e(k)) = J(k) - J(k-1) < 0 \tag{39}$$

From this, the convergence of $J(k)$ to 0 occurs when k increases into infinity. Meanwhile, $u[k] = u^*$ is applied for all k but the weighting matrix, W is selected to satisfy

$$W - A^T WA > 0 \tag{40}$$

The following theorem can be used to support the above argument:

Theorem 1: Based on the discrete-time of the system, the CCS-MPC presented in (34) can guarantee the stability of the closed-loop at constant reference torque T_e^* when the reference state x^* has a convenient steady-state input u^* besides the better selection for all gains and the value of *the weighting matrix W* [54].

Proof: Under this assumption, the value of the cost index $J(k)$ decreases dramatically as (39). Hence, the value of $x\,[k]$ converge to x^* at k reaches to infinity.

Remark 1: The reference state x^* of the reference torque T_e^* is determined based on the dynamic model of the machine following the other remaining procedures. From the other remaining procedures other, the most important value is determined thus x^* has a convenient steady-state input u^* based on the operating mode.

VIII. CONCLUSION

The MPC is becoming one popular and effective technique to achieve high drive performance in electrical machines and systems. This paper has provided a comprehensive state of the art for applying MPC techniques in electric machines and systems. As one of the main focuses in this work, it fully discusses the control strategies without any attention to the type of the electric machine and how these control strategies solve the problems associated with the MPC. In general, the FCS-MPC, CCS-MPC, and FCS-MPDTC with optimum duty ratio have been presented for electric drives in this work. Meanwhile, the issues and solutions for these control techniques have been discussed in details with great focus on experimental results based on different kinds of machines and drives.

Despite many researchers have developed the MPC with different techniques, but there are still some serious issues for the MPC to be urgently solved in near future, e.g., how to improve the electrical drive performance by employing some simplified MPCs with low computation time, low parameter dependence, fast dynamics, and so on. Furthermore, the stability analysis for the MPC should be studied. Fortunately, at the same time, as the rapid technology evolution of the microcontrollers and digital signal processors, and so on, the MPC would find more and more opportunities for the industrial applications. Further in-depth research on Online optimization of weighting factors, cost index without weighting factors, MPC in multi-phase machines and multi-inverters, integrating different types of MPCs with other techniques such as adaptive sliding mode, the use of the MPC for energy management and regenerative braking in EVs/HEVs, sensorless-based MPCs, and the dependence of the MPC for grid-connected power inverters with multi renewable energy sources, i.e. wind, PV, battery, fuel cells, and diesel may increase the functionality of the MPC and may fulfil the modern industrial demand.

APPENDIX

TABLE 6. Main parameters of the aim.

Parameter	Symbol	Value	Unit
Secondary resistance	R_2	2.4	Ω
Rated thrust	F_r	280	N
Pole pitch length	τ	0.1485	m
Secondary leakage inductance	L_{l1}	11.09	mH
Rated speed	V_r	11	m/s
Primary resistance	R_1	1	Ω
Primary length	D_s	1.3087	m
Primary leakage inductance	L_{l2}	3.82	mH
Rated power	P_r	3	kW

REFERENCES

[1] E. Camacho and C. Bordons, *Model Predictive Control*. Berlin, Germany: Springer-Verlag, 1999.

[2] J. Holtz and S. Stadtfeld, "A predictive controller for the stator current vector of ac machines fed from a switched voltage source," in *Proc. IPEC*, 1983, pp. 1665–1675.

[3] J. Rodriguez, M. P. Kazmierkowski, J. R. Espinoza, P. Zanchetta, H. Abu-Rub, H. A. Young, and C. A. Rojas, "State of the art of finite control set model predictive control in power electronics," *IEEE Trans. Ind. Informat.*, vol. 9, no. 2, pp. 1003–1016, May 2013.

[4] X. Zhang and Y. He, "Direct voltage-selection based model predictive direct speed control for PMSM drives without weighting factor," *IEEE Trans. Power Electron.*, vol. 34, no. 8, pp. 7838–7851, Aug. 2019.

[5] Z. Zhou, C. Xia, Y. Yan, Z. Wang, and T. Shi, "Torque ripple minimization of predictive torque control for PMSM with extended control set," *IEEE Trans. Ind. Electron.*, vol. 64, no. 9, pp. 6930–6939, Sep. 2017.

[6] J. Rodriguez and P. Cortes, *Predictive Control of Power Converters and Electrical Drives*. Hoboken, NJ, USA: Wiley, 2012.

[7] Y. Zhang and H. Yang, "Model-predictive flux control of induction motor drives with switching instant optimization," *IEEE Trans. Energy Convers.*, vol. 30, no. 3, pp. 1113–1122, Sep. 2015.

[8] R. H. Kumar, A. Iqbal, and N. C. Lenin, "Review of recent advancements of direct torque control in induction motor drives—A decade of progress," *IET Power Electron.*, vol. 11, no. 1, pp. 1–15, Jan. 2018.

[9] S.-D. Huang, G.-Z. Cao, J. Xu, Y. Cui, C. Wu, and J. He, "Predictive position control of long-stroke planar motors for high-precision positioning applications," *IEEE Trans. Ind. Electron.*, vol. 68, no. 1, pp. 796–811, Jan. 2021.

[10] Z. Zheng, D. Sun, M. Wang, and H. Nian, "A dual two-vector-based model predictive flux control with field-weakening operation for OW-PMSM drives," *IEEE Trans. Power Electron.*, vol. 36, no. 2, pp. 2191–2200, Feb. 2021.

[11] F. Wang, G. Lin, and Y. He, "Passivity-based model predictive control of three-level inverter-fed induction motor," *IEEE Trans. Power Electron.*, vol. 36, no. 2, pp. 1984–1993, Feb. 2021.

[12] B. Cao, B. M. Grainger, X. Wang, Y. Zou, G. F. Reed, and Z.-H. Mao, "Direct torque model predictive control of a five-phase permanent magnet synchronous motor," *IEEE Trans. Power Electron.*, vol. 36, no. 2, pp. 2346–2360, Feb. 2021.

[13] J. Hang, H. Wu, J. Zhang, S. Ding, Y. Huang, and W. Hua, "Cost function-based open-phase fault diagnosis for PMSM drive system with model predictive current control," *IEEE Trans. Power Electron.*, vol. 36, no. 3, pp. 2574–2583, Mar. 2021.

[14] S. G. Petkar, K. Eshwar, and V. K. Thippiripati, "A modified model predictive current control of permanent magnet synchronous motor drive," *IEEE Trans. Ind. Electron.*, vol. 68, no. 2, pp. 1025–1034, Feb. 2021.

[15] M. Bermudez, M. R. Arahal, M. J. Duran, and I. Gonzalez-Prieto, "Model predictive control of six-phase electric drives including ARX disturbance estimator," *IEEE Trans. Ind. Electron.*, vol. 68, no. 1, pp. 81–91, Jan. 2021.

[16] F. Wang and L. He, "FPGA-based predictive speed control for PMSM system using integral sliding-mode disturbance observer," *IEEE Trans. Ind. Electron.*, vol. 68, no. 2, pp. 972–981, Feb. 2021.
[17] Y. Zhang, J. Jin, and L. Huang, "Model-free predictive current control of PMSM drives based on extended state observer using ultralocal model," *IEEE Trans. Ind. Electron.*, vol. 68, no. 2, pp. 993–1003, Feb. 2021.
[18] S. A. Davari, V. Nekoukar, C. Garcia, and J. Rodriguez, "Online weighting factor optimization by simplified simulated annealing for finite set predictive control," *IEEE Trans. Ind. Informat.*, vol. 17, no. 1, pp. 31–40, Jan. 2021.
[19] D. F. Valencia, R. Tarvirdilu-Asl, C. Garcia, J. Rodriguez, and A. Emadi, "A review of predictive control techniques for switched reluctance machine drives. Part II: Torque control, assessment and challenges," *IEEE Trans. Energy Convers.*, early access, Dec. 29, 2021, doi: 10.1109/TEC.2020.3047981.
[20] A. A. Ahmed, B. K. Koh, and Y. I. Lee, "A comparison of finite control set and continuous control set model predictive control schemes for speed control of induction motors," *IEEE Trans. Ind. Informat.*, vol. 14, no. 4, pp. 1334–1346, Apr. 2018.
[21] M. Preindl and S. Bolognani, "Model predictive direct torque control with finite control set for PMSM drive systems, Part 1: Maximum torque per ampere operation," *IEEE Trans. Ind. Informat.*, vol. 9, no. 4, pp. 1912–1921, Nov. 2013.
[22] Y. Zhang, B. Zhang, H. Yang, M. Norambuena, and J. Rodriguez, "Generalized sequential model predictive control of IM drives with field-weakening ability," *IEEE Trans. Power Electron.*, vol. 34, no. 9, pp. 8944–8955, Sep. 2019.
[23] A. Devanshu, M. Singh, and N. Kumar, "An improved nonlinear flux observer based sensorless FOC IM drive with adaptive predictive current control," *IEEE Trans. Power Electron.*, vol. 35, no. 1, pp. 652–666, Jan. 2020.
[24] F. Qi, A. Stippich, I. Ralev, A. Klein-Hessling, and R. W. De Doncker, "Model predictive control of a switched reluctance machine for guaranteed overload torque," *IEEE Trans. Ind. Appl.*, vol. 55, no. 2, pp. 1321–1331, Mar. 2019.
[25] E. Garayalde, I. Aizpuru, U. Iraola, I. Sanz, C. Bernal, and E. Oyarbide, "Finite control set MPC vs continuous control set MPC performance comparison for synchronous buck converter control in energy storage application," in *Proc. Int. Conf. Clean Electr. Power (ICCEP)*, Otranto, Italy, Jul. 2019, pp. 490–495.
[26] F. Ramirez and M. Pacas, "Finite control set model based predictive control of a PMSM with variable switching frequency and torque ripple optimization," in *Proc. Int. Exhib. Conf. Power Electron. Intell. Motion, Renew. Energy Energy Manage.*, Nuremberg, Germany, 2016, pp. 1–8.
[27] F. Wang, X. Mei, J. Rodriguez, and R. Kennel, "Model predictive control for electrical drive systems—An overview," *CES Trans. Electr. Mach. Syst.*, vol. 1, no. 3, pp. 219–230, Sep. 2017.
[28] Z. Zhou, C. Xia, T. Shi, and Q. Geng, "Model predictive direct duty-cycle control for PMSM drive systems with variable control set," *IEEE Trans. Ind. Electron.*, vol. 68, no. 4, pp. 2976–2987, Apr. 2021.
[29] M. Habibullah, D. D.-C. Lu, D. Xiao, and M. F. Rahman, "Finite-state predictive torque control of induction motor supplied from a three-level NPC voltage source inverter," *IEEE Trans. Power Electron.*, vol. 32, no. 1, pp. 479–489, Jan. 2017.
[30] M. Habibullah, D. D.-C. Lu, D. Xiao, I. Osman, and M. F. Rahman, "Selected prediction vectors based FS-PTC for 3L-NPC inverter fed motor drives," *IEEE Trans. Ind. Appl.*, vol. 53, no. 4, pp. 3588–3597, Jul./Aug. 2017.
[31] M. Mamdouh, M. A. Abido, and Z. Hamouz, "Weighting factor selection techniques for predictive torque control of induction motor drives: A comparison study," *Arabian J. Sci. Eng.*, vol. 43, no. 2, pp. 433–445, Feb. 2018.
[32] F. Wang, S. Li, X. Mei, W. Xie, J. Rodriguez, and R. M. Kennel, "Model-based predictive direct control strategies for electrical drives: An experimental evaluation of PTC and PCC methods," *IEEE Trans. Ind. Informat.*, vol. 11, no. 3, pp. 671–681, Jun. 2015.
[33] J. Zou, W. Xu, X. Yu, Y. Liu, and C. Ye, "Multistep model predictive control with current and voltage constraints for linear induction machine based urban transportation," *IEEE Trans. Veh. Technol.*, vol. 66, no. 12, pp. 10817–10829, Dec. 2017.
[34] W. Xu, J. Zou, Y. Liu, and J. Zhu, "Weighting factorless model predictive thrust control for linear induction machine," *IEEE Trans. Power Electron.*, vol. 34, no. 10, pp. 9916–9928, Oct. 2019.
[35] R. Zhang, B. Xia, H. Yang, and J. Rodriguez, "Overview of model predictive control for induction motor drives," *Chin. J. Electr. Eng.*, vol. 2, no. 1, pp. 62–76, Jun. 2019.
[36] Y. Wang, W. Xie, X. Wang, W. Yang, M. Dou, S. Song, and D. Gerling, "Fast response model predictive torque and flux control with low calculation effort for PMSMs," *IEEE Trans. Ind. Informat.*, vol. 15, no. 10, pp. 5531–5540, Oct. 2019.
[37] M. Kashif, S. Murshid, and B. Singh, "Continuous control set model predictive controller for PMSM driven solar PV water pumping system," in *Proc. IEEE Int. Conf. Environ. Electr. Eng., IEEE Ind. Commercial Power Syst. Eur. (EEEIC/I&CPS Europe)*, Genova, Italy, Jun. 2019, pp. 1–6.
[38] M. F. Elmorshedy, W. Xu, Y. Liu, S. M. Allam, and M. Dong, "Speed control of linear induction motor based on finite-set model predictive direct flux control," in *Proc. IEEE Int. Symp. Predictive Control Elect. Drives Power Electron. (PRECEDE)*, Quanzhou, China, May 2019, pp. 1–6.
[39] J. Zou, W. Xu, J. Zhu, and Y. Liu, "Low-complexity finite control set model predictive control with current limit for linear induction machines," *IEEE Trans. Ind. Electron.*, vol. 65, no. 12, pp. 9243–9254, Dec. 2018.
[40] L. Yan, F. Wang, M. Dou, Z. Zhang, R. Kennel, and J. Rodriguez, "Active disturbance-rejection-based speed control in model predictive control for induction machines," *IEEE Trans. Ind. Electron.*, vol. 67, no. 4, pp. 2574–2584, Apr. 2020.
[41] X. Yuan, S. Zhang, and C. Zhang, "Improved model predictive current control for SPMSM drives with parameter mismatch," *IEEE Trans. Ind. Electron.*, vol. 67, no. 2, pp. 852–862, Feb. 2020.
[42] O. Sandre-Hernandez, J. Rangel-Magdaleno, and R. Morales-Caporal, "A comparison on finite-set model predictive torque control schemes for PMSMs," *IEEE Trans. Power Electron.*, vol. 33, no. 10, pp. 8838–8847, Oct. 2018.
[43] G. Li, J. Hu, Y. Li, and J. Zhu, "An improved model predictive direct torque control strategy for reducing harmonic currents and torque ripples of five-phase permanent magnet synchronous motors," *IEEE Trans. Ind. Electron.*, vol. 66, no. 8, pp. 5820–5829, Aug. 2019.
[44] F. Mwasilu, H. T. Nguyen, H. H. Choi, and J.-W. Jung, "Finite set model predictive control of interior PM synchronous motor drives with an external disturbance rejection technique," *IEEE/ASME Trans. Mechatronics*, vol. 22, no. 2, pp. 762–773, Apr. 2017.
[45] Y. Luo and C. Liu, "Model predictive control for a six-phase PMSM motor with a reduced-dimension cost function," *IEEE Trans. Ind. Electron.*, vol. 67, no. 2, pp. 969–979, Feb. 2020.
[46] Y. Nie, D. C. Ludois, and I. P. Brown, "Deadbeat-direct torque and flux control of wound field synchronous machine at low sampling to fundamental frequency ratios," *IEEE Trans. Ind. Appl.*, vol. 55, no. 4, pp. 3813–3822, Jul. 2019.
[47] M. Abdelrahem, C. M. Hackl, R. Kennel, and J. Rodriguez, "Computationally efficient finite-position-set-phase-locked loop for sensorless control of PMSGs in wind turbine applications," *IEEE Trans. Power Electron.*, vol. 36, no. 3, pp. 3007–3016, Mar. 2021.
[48] C. Xue, D. Zhou, and Y. Li, "Finite-control-set model predictive control for three-level NPC inverter-fed PMSM drives with LC filter," *IEEE Trans. Ind. Electron.*, early access, Dec. 8, 2020, doi: 10.1109/TIE.2020.3042156.
[49] M. Mousavi, A. Davari, V. Nekoukar, C. Garcia, and J. Rodriguez, "A robust torque and flux prediction model by a modified disturbance rejection method for finite set model predictive control of induction motor," *IEEE Trans. Power Electron.*, early access, Jan. 25, 2021, doi: 10.1109/TPEL.2021.3054242.
[50] K. Bandy and P. Stumpf, "Model predictive torque control for multilevel inverter fed induction machines using sorting networks," *IEEE Access*, vol. 9, pp. 13800–13813, 2021.
[51] W. Xu, M. F. Elmorshedy, Y. Liu, J. Rodriguez, and C. Garcia, "Maximum thrust per ampere of linear induction machine based on finite-set model predictive direct thrust control," *IEEE Trans. Power Electron.*, vol. 35, no. 7, pp. 7366–7378, Jul. 2020.
[52] Y. Zhang, Z. Yin, W. Li, J. Liu, and Y. Zhang, "Adaptive sliding-mode-based speed control in finite control set model predictive torque control for induction motors," *IEEE Trans. Power Electron.*, vol. 36, no. 7, pp. 8076–8087, Jul. 2021.

[53] D.-K. Choi and K.-B. Lee, "Dynamic performance improvement of AC/DC converter using model predictive direct power control with finite control set," *IEEE Trans. Ind. Electron.*, vol. 62, no. 2, pp. 757–767, Feb. 2015.

[54] A. A. Ahmed, B. K. Koh, and Y. I. Lee, "Continuous control set-model predictive control for torque control of induction motors in a wide speed range," *Electr. Power Compon. Syst.*, vol. 46, nos. 19–20, pp. 2142–2158, Dec. 2018.

[55] P. V. Harisyam, V. Prasanth, V. Natarajan, and K. Basu, "Continuous control set model predictive control of buck converter," in *Proc. 46th Annu. Conf. IEEE Ind. Electron. Soc. (IECON)*, Singapore, Oct. 2020, pp. 1297–1302.

[56] F. Toso, P. G. Carlet, A. Favato, and S. Bolognani, "On-line continuous control set MPC for PMSM drives current loops at high sampling rate using qpOASES," in *Proc. IEEE Energy Convers. Congr. Expo. (ECCE)*, Baltimore, MD, USA, Sep. 2019, pp. 6615–6620.

[57] A. Favato, P. G. Carlet, F. Toso, and S. Bolognani, "A novel formulation of continuous control set MPC for induction motor drives," in *Proc. IEEE Int. Conf. Electr. Mach. Drives (IEMDC)*, San Diego, CA, USA, May 2019, pp. 2196–2202.

[58] P. G. Carlet, F. Toso, A. Favato, and S. Bolognani, "A speed and current cascade continuous control set model predictive control architecture for synchronous motor drives," in *Proc. IEEE Energy Convers. Congr. Expo. (ECCE)*, Baltimore, MD, USA, Sep. 2019, pp. 5682–5688.

[59] Y. Zhang and H. Yang, "Model predictive torque control of induction motor drives with optimal duty cycle control," *IEEE Trans. Power Electron.*, vol. 29, no. 12, pp. 6593–6603, Dec. 2014.

[60] E. Fuentes, C. A. Silva, and R. M. Kennel, "MPC implementation of a quasi-time-optimal speed control for a PMSM drive, with inner Modulated-FS-MPC torque control," *IEEE Trans. Ind. Electron.*, vol. 63, no. 6, pp. 3897–3905, Jun. 2016.

[61] M. R. Nikzad, B. Asaei, and S. O. Ahmadi, "Discrete duty-cycle-control method for direct torque control of induction motor drives with model predictive solution," *IEEE Trans. Power Electron.*, vol. 33, no. 3, pp. 2317–2329, Mar. 2018.

[62] L. Yan, M. Dou, and Z. Hua, "Disturbance compensation-based model predictive flux control of SPMSM with optimal duty cycle," *IEEE J. Emerg. Sel. Topics Power Electron.*, vol. 7, no. 3, pp. 1872–1882, Sep. 2019.

[63] Y. Zhang and H. Yang, "Torque ripple reduction of model predictive torque control of induction motor drives," in *Proc. IEEE Energy Convers. Congr. Expo.*, Denver, CO, USA, Sep. 2013, pp. 1176–1183.

[64] Y. Ren, Z. Q. Zhu, and J. Liu, "Direct torque control of permanent-magnet synchronous machine drives with a simple duty ratio regulator," *IEEE Trans. Ind. Electron.*, vol. 61, no. 10, pp. 5249–5258, Oct. 2014.

[65] Q. Liu and K. Hameyer, "Torque ripple minimization for direct torque control of PMSM with modified FCSMPC," *IEEE Trans. Ind. Appl.*, vol. 52, no. 6, pp. 4855–4864, Nov. 2016.

[66] Y. Zhang and J. Zhu, "Direct torque control of permanent magnet synchronous motor with reduced torque ripple and commutation frequency," *IEEE Trans. Power Electron.*, vol. 26, no. 1, pp. 235–248, Jan. 2011.

[67] M. Amiri, J. Milimonfared, and D. A. Khaburi, "Predictive torque control implementation for induction motors based on discrete space vector modulation," *IEEE Trans. Ind. Electron.*, vol. 65, no. 9, pp. 6881–6889, Sep. 2018.

[68] X. Wu, W. Song, and C. Xue, "Low-complexity model predictive torque control method without weighting factor for five-phase PMSM based on hysteresis comparators," *IEEE J. Emerg. Sel. Topics Power Electron.*, vol. 6, no. 4, pp. 1650–1661, Dec. 2018.

[69] A. A. Ahmed, B. K. Koh, H. S. Park, K.-B. Lee, and Y. I. Lee, "Finite-control set model predictive control method for torque control of induction motors using a state tracking cost index," *IEEE Trans. Ind. Electron.*, vol. 64, no. 3, pp. 1916–1928, Mar. 2017.

[70] A. Mora, A. Orellana, J. Juliet, and R. Cardenas, "Model predictive torque control for torque ripple compensation in variable-speed PMSMs," *IEEE Trans. Ind. Electron.*, vol. 63, no. 7, pp. 4584–4592, Jul. 2016.

[71] M. Safaeian, A. Jalilvand, and A. Taheri, "A MRAS based model predictive control for multi-leg based multi-drive system used in hot rolling mill applications," *IEEE Access*, vol. 8, pp. 215493–215504, 2020.

[72] K. Bandy and P. Stumpf, "Model predictive torque control for multilevel inverter fed induction machines using sorting networks," *IEEE Access*, vol. 9, pp. 13800–13813, Jan. 2021.

[73] C. A. Rojas, J. Rodriguez, F. Villarroel, J. R. Espinoza, C. A. Silva, and M. Trincado, "Predictive torque and flux control without weighting factors," *IEEE Trans. Ind. Electron.*, vol. 60, no. 2, pp. 681–690, Feb. 2013.

[74] Z. Song, Y. Wang, and T. Shi, "A dual-loop predictive control structure for permanent magnet synchronous machines with enhanced attenuation of periodic disturbances," *IEEE Trans. Power Electron.*, vol. 35, no. 1, pp. 760–774, Jan. 2020.

[75] P. Cortes, S. Kouro, B. La Rocca, R. Vargas, J. Rodriguez, J. I. Leon, S. Vazquez, and L. G. Franquelo, "Guidelines for weighting factors design in model predictive control of power converters and drives," in *Proc. IEEE Int. Conf. Ind. Technol.*, Gippsland, VIC, Australia, Feb. 2009, pp. 1–7.

[76] T. J. Vyncke, S. Thielemans, T. Dierickx, R. Dewitte, M. Jacxsens, and J. A. Melkebeek, "Design choices for the prediction and optimization stage of finite-set model based predictive control," in *Proc. Workshop Predictive Control Elect. Drives Power Electron.*, Munich, Germany, 2011, pp. 47–54.

[77] F. Villarroel, J. R. Espinoza, C. A. Rojas, J. Rodriguez, M. Rivera, and D. Sbarbaro, "Multiobjective switching state selector for finite-states model predictive control based on fuzzy decision making in a matrix converter," *IEEE Trans. Ind. Electron.*, vol. 60, no. 2, pp. 589–599, Feb. 2013.

[78] S. A. Davari, D. A. Khaburi, and R. Kennel, "An improved FCS–MPC algorithm for an induction motor with an imposed optimized weighting factor," *IEEE Trans. Power Electron.*, vol. 27, no. 3, pp. 1540–1551, Mar. 2012.

[79] C. A. Rojas, J. R. Rodriguez, S. Kouro, and F. Villarroel, "Multiobjective fuzzy-decision-making predictive torque control for an induction motor drive," *IEEE Trans. Power Electron.*, vol. 32, no. 8, pp. 6245–6260, Aug. 2017.

[80] T. Dragicevic and M. Novak, "Weighting factor design in model predictive control of power electronic converters: An artificial neural network approach," *IEEE Trans. Ind. Electron.*, vol. 66, no. 11, pp. 8870–8880, Nov. 2019.

[81] S. A. Davari, D. A. Khaburi, and R. Kennel, "An improved FCS–MPC algorithm for an induction motor with an imposed optimized weighting factor," *IEEE Trans. Power Electron.*, vol. 27, no. 3, pp. 1540–1551, Mar. 2012.

[82] V. P. Muddineni, S. R. Sandepudi, and A. K. Bonala, "Improved weighting factor selection for predictive torque control of induction motor drive based on a simple additive weighting method," *Electr. Power Compon. Syst.*, vol. 45, no. 13, pp. 1450–1462, Nov. 2017.

[83] M. Norambuena, J. Rodriguez, Z. Zhang, F. Wang, C. Garcia, and R. Kennel, "A very simple strategy for high-quality performance of AC machines using model predictive control," *IEEE Trans. Power Electron.*, vol. 34, no. 1, pp. 794–800, Jan. 2019.

[84] M. Mamdouh and M. A. Abido, "Efficient predictive torque control for induction motor drive," *IEEE Trans. Ind. Electron.*, vol. 66, no. 9, pp. 6757–6767, Sep. 2019.

[85] F. Wang, H. Xie, Q. Chen, S. A. Davari, J. Rodriguez, and R. Kennel, "Parallel predictive torque control for induction machines without weighting factors," *IEEE Trans. Power Electron.*, vol. 35, no. 2, pp. 1779–1788, Feb. 2020.

[86] V. P. Muddineni, S. R. Sandepudi, and A. K. Bonala, "Simplified finite control set model predictive control for induction motor drive without weighting factors," in *Proc. IEEE Int. Conf. Power Electron., Drives Energy Syst. (PEDES)*, Trivandrum, India, Dec. 2016, pp. 1–6.

[87] S. A. Davari and J. Rodriguez, "Predictive direct voltage control of induction motor with mechanical model consideration for sensorless applications," *IEEE J. Emerg. Sel. Topics Power Electron.*, vol. 6, no. 4, pp. 1990–2000, Dec. 2018.

[88] Y. Zhang, H. Yang, and B. Xia, "Model-predictive control of induction motor drives: Torque control versus flux control," *IEEE Trans. Ind. Appl.*, vol. 52, no. 5, pp. 4050–4060, Sep. 2016.

[89] X. Mei, R. Zu, F. Wang, and R. Kennel, "Variable cost functions' sequence design for model predictive control of IPMSM without weighting factor," in *Proc. IEEE Int. Conf. Inf. Autom. (ICIA)*, Wuyishan, China, Aug. 2018, pp. 500–505.

[90] L. Guo, K. Zhang, N. Jin, L. Cao, K. Luo, and H. Wang, "Dynamic cost function based predictive torque control for permanent magnet synchronous motor without using weighting factor," in *Proc. IEEE Int. Power Electron. Appl. Conf. Expo. (PEAC)*, Shenzhen, China, Nov. 2018, pp. 1–5.

[91] L. Guo, X. Zhang, S. Yang, Z. Xie, L. Wang, and R. Cao, "Simplified model predictive direct torque control method without weighting factors for permanent magnet synchronous generator-based wind power system," *IET Electr. Power Appl.*, vol. 11, no. 5, pp. 793–804, May 2017.
[92] D. Wu, J. Chen, R. Zhu, and G. Hua, "Simplified model predictive flux control for dual inverter fed open end winding induction motor," in *Proc. IEEE Int. Symp. Power Electron. Distrib. Gener. Syst. (PEDG)*, Xi'an, China, Jun. 2019, pp. 1050–1054.
[93] M. F. Elmorshedy, W. Xu, S. M. Allam, J. Rodriguez, and C. Garcia, "MTPA-based finite-set model predictive control without weighting factors for linear induction machine," *IEEE Trans. Ind. Electron.*, vol. 68, no. 3, pp. 2034–2047, Mar. 2021.
[94] Y. Zhang, H. Yang, and B. Xia, "Model predictive torque control of induction motor drives with reduced torque ripple," *IET Electr. Power Appl.*, vol. 9, no. 9, pp. 595–604, Nov. 2015.
[95] M. H. Arshad, M. A. Abido, A. Salem, and A. H. Elsayed, "Weighting factors optimization of model predictive torque control of induction motor using NSGA-II with TOPSIS decision making," *IEEE Access*, vol. 7, pp. 177595–177606, Dec. 2019.
[96] W. Kong, J. Ding, T. Chai, and J. Sun, "Large-dimensional multi-objective evolutionary algorithms based on improved average ranking," in *Proc. 49th IEEE Conf. Decis. Control (CDC)*, Atlanta, GA, USA, Dec. 2010, pp. 502–507.
[97] R. O. Ramirez, C. R. Baier, F. Villarroel, J. R. Espinoza, J. Pou, and J. Rodriguez, "A hybrid FCS-MPC with low and fixed switching frequency without steady-state error applied to a grid-connected CHB inverter," *IEEE Access*, vol. 8, pp. 223637–223651, 2020.
[98] W. Xu, M. F. Elmorshedy, Y. Liu, M. R. Islam, and S. M. Allam, "Finite-set model predictive control based thrust maximization of linear induction motors used in linear metros," *IEEE Trans. Veh. Technol.*, vol. 68, no. 6, pp. 5443–5458, Jun. 2019.
[99] M. Preindl and S. Bolognani, "Model predictive direct torque control with finite control set for PMSM drive systems, Part 2: Field weakening operation," *IEEE Trans. Ind. Informat.*, vol. 9, no. 2, pp. 648–657, May 2013.
[100] S. A. Davari, "Predictive direct angle control of induction motor," *IEEE Trans. Ind. Electron.*, vol. 63, no. 8, pp. 5276–5284, Aug. 2016.
[101] D. Ye, J. Li, R. Qu, H. Lu, and Y. Lu, "Finite set model predictive MTPA control with VSD method for asymmetric six-phase PMSM," in *Proc. IEEE Int. Electr. Mach. Drives Conf. (IEMDC)*, Miami, FL, USA, May 2017, pp. 1–7.
[102] G. Liu, C. Song, and Q. Chen, "FCS-MPC-based fault-tolerant control of five-phase IPMSM for MTPA operation," *IEEE Trans. Power Electron.*, vol. 35, no. 3, pp. 2882–2894, Mar. 2020.
[103] J. Thomas and A. Hansson, "Speed tracking of a linear induction motor-enumerative nonlinear model predictive control," *IEEE Trans. Control Syst. Technol.*, vol. 21, no. 5, pp. 1956–1962, Sep. 2013.
[104] Y. Zhang and H. Yang, "Two-vector-based model predictive torque control without weighting factors for induction motor drives," *IEEE Trans. Power Electron.*, vol. 31, no. 2, pp. 1381–1390, Feb. 2016.
[105] R. Errouissi, M. Ouhrouche, W.-H. Chen, and A. M. Trzynadlowski, "Robust nonlinear predictive controller for permanent-magnet synchronous motors with an optimized cost function," *IEEE Trans. Ind. Electron.*, vol. 59, no. 7, pp. 2849–2858, Jul. 2012.
[106] S. Chai, L. Wang, and E. Rogers, "A cascade MPC control structure for a PMSM with speed ripple minimization," *IEEE Trans. Ind. Electron.*, vol. 60, no. 8, pp. 2978–2987, Aug. 2013.
[107] C. Garcia, J. Rodriguez, C. Silva, C. Rojas, P. Zanchetta, and H. Abu-Rub, "Cascaded predictive speed control," in *Proc. 40th Annu. Conf. IEEE Ind. Electron. Soc. (IECON)*, Dallas, TX, USA, Oct. 2014, pp. 3824–3830.
[108] E. J. Fuentes, C. A. Silva, and J. I. Yuz, "Predictive speed control of a two-mass system driven by a permanent magnet synchronous motor," *IEEE Trans. Ind. Electron.*, vol. 59, no. 7, pp. 2840–2848, Jul. 2012.
[109] E. Fuentes, D. Kalise, J. Rodriguez, and R. M. Kennel, "Cascade-free predictive speed control for electrical drives," *IEEE Trans. Ind. Electron.*, vol. 61, no. 5, pp. 2176–2184, May 2014.
[110] X. Zhang, Y. He, Y. Li, and Y. Zhang, "Double vector model predictive direct speed control without weighting factor," in *Proc. 21st Int. Conf. Electr. Mach. Syst. (ICEMS)*, Jeju, South Korea, Oct. 2018, pp. 1446–1449.
[111] X. Gao, M. Abdelrahem, C. M. Hackl, Z. Zhang, and R. Kennel, "Direct predictive speed control with a sliding manifold term for PMSM drives," *IEEE J. Emerg. Sel. Topics Power Electron.*, vol. 8, no. 2, pp. 1258–1267, Jun. 2020.
[112] J. Yang, H. Wu, L. Hu, and S. Li, "Robust predictive speed regulation of converter-driven DC motors via a discrete-time reduced-order GPIO," *IEEE Trans. Ind. Electron.*, vol. 66, no. 10, pp. 7893–7903, Oct. 2019.
[113] M. Liu, K. W. Chan, J. Hu, W. Xu, and J. Rodriguez, "Model predictive direct speed control with torque oscillation reduction for PMSM drives," *IEEE Trans. Ind. Informat.*, vol. 15, no. 9, pp. 4944–4956, Sep. 2019.

MAHMOUD F. ELMORSHEDY (Member, IEEE) was born in Gharbeya, Egypt, in 1989. He received the B.Sc. and M.Sc. degrees in electrical engineering from Tanta University, Egypt, in 2012 and 2016, respectively, and the Ph.D. degree in electrical engineering from the School of Electrical and Electronic Engineering, Huazhong University of Science and Technology, China, in 2020. He started working as a Teaching Assistant with the Department of Electrical Power and Machines Engineering, Faculty of Engineering, Tanta University, in 2013, where he was promoted to an Assistant Lecturer, in June 2016. He is currently working as an Assistant Professor with the Department of Electrical Power and Machines Engineering, Faculty of Engineering, Tanta University. His research interests include linear induction motor, predictive control, power electronics, and renewable energy.

WEI XU (Senior Member, IEEE) received the B.E. and M.E. degrees in electrical engineering from Tianjin University, Tianjin, China, in 2002 and 2005, respectively, and the Ph.D. degree in electrical engineering from the Institute of Electrical Engineering, Chinese Academy of Sciences, in 2008.

From 2008 to 2012, he was a Postdoctoral Fellow with the University of Technology Sydney, a Vice Chancellor Research Fellow with the Royal Melbourne Institute of Technology, and a Japan Science Promotion Society Invitation Fellow with Meiji University, respectively. Since 2013, he has been a Full Professor with the State Key Laboratory of Advanced Electromagnetic Engineering, Huazhong University of Science and Technology, China. He has more than 110 articles accepted or published in IEEE journals, two edited books published by Springer Press, one monograph published by China Machine Press, and more than 150 invention patents granted or in pending, all in the related fields of electrical machines and drives. His research interest includes design and control of linear/rotary machines. He is a Fellow of the Institute of Engineering and Technology (IET). He will serve as the General Chair for 2021 International Symposium on Linear Drives for Industry Applications (LDIA 2021) and 2023 IEEE International Conference on Predictive Control of Electrical Drives and Power Electronics (PRECEDE 2023) in Wuhan, China, respectively. He has served as an Associate Editor for several leading IEEE Transactions journals, such as IEEE Transactions on Industrial Electronics, IEEE Transactions on Vehicular Technology, and IEEE Transactions on Energy Conversion.

FAYEZ F. M. EL-SOUSY (Member, IEEE) received the B.Sc. degree in electrical engineering from Menoufia University, Egypt in 1988, and the M.Sc. and Ph.D. degrees in electrical engineering from Cairo University, Giza, Egypt, in 1994 and 2000, respectively. From August 1995 to June 2000, he was a Lecturer with the Department of Electrical Engineering, October Six University, Giza. From August 2000 to June 2003, he was an Assistant Professor with the Department of Electrical Engineering, October Six University. From April 2004 to February 2007, he was a Postdoctoral Visiting Researcher with the Graduate School of Information Science and Electrical Engineering, Kyushu University, Fukuoka, Japan. From 2007 to 2010, he was an Associate Professor and the Chair of the Electrical Engineering Department, College of Engineering, King Saud University, Riyadh, Saudi Arabia. From 2010 to 2014, he was an Associate Professor and the Chair of the Electrical Engineering Department, College of Engineering, Salman Bin Abdulaziz University, Al-Kharj, Saudi Arabia. Since 2014, he has been a Full Professor and the Chair with the Electrical Engineering Department, College of Engineering, Prince Sattam Bin Abdulaziz University, Saudi Arabia. His research interests include modeling and control of motor drives, motion-control systems, wind energy systems, digital signal processing-based computer control systems, computational intelligent of power electronics, electric drives and power systems, intelligent control theories including fuzzy logic, neural networks, and wavelets, nonlinear control, optimal control, and robust control.

MD. RABIUL ISLAM (Senior Member, IEEE) received the Ph.D. degree in electrical engineering from the University of Technology Sydney (UTS), Sydney, Australia, in 2014.

He was appointed a Lecturer with RUET, in 2005, and promoted to a Full Professor in 2017. He joined the School of Electrical, Computer, and Telecommunications Engineering (SECTE), University of Wollongong (UOW), Wollongong, Australia, in 2018. He has authored or coauthored more than 200 articles, including 53 IEEE TRANSACTIONS/IEEE journal articles. He has written or edited five technical books published by Springer and Taylor & Francis. His research interests include power electronic converters, renewable energy technologies, power quality, electrical machines, electric vehicles, and smart grid. He has received several Best Paper Awards, including two Best Paper recognitions from the IEEE TRANSACTIONS ON ENERGY CONVERSION in 2020. He has served as a Guest Editor for IEEE TRANSACTIONS ON ENERGY CONVERSION, IEEE TRANSACTIONS ON APPLIED SUPERCONDUCTIVITY, and *IET Electric Power Applications*. He has been serving as an Editor for IEEE TRANSACTIONS ON ENERGY CONVERSION and the IEEE POWER ENGINEERING LETTERS, and an Associate Editor for IEEE ACCESS. He has received several funding from Government and Industries including Australian Government ARC Discovery Project 2020 entitled A Next Generation Smart Solid-State Transformer for Power Grid Applications.

ABDELSALAM A. AHMED was born in Kafrelsheikh, Egypt. He graduated from Tanta University, Egypt, in 2002. He received the M.S. degree from Tanta University, in 2008, and the Ph.D. degree in electrical engineering and automation from the Harbin Institute of Technology, China, in 2012. From July 2013 to July 2014, he was a Postdoctoral Fellowship with the Department of Instrumental Science and Technology, School of Electrical Engineering and Automation, Harbin Institute of Technology. From September 2015 to September 2016, he was a Postdoctoral Fellowship with the Department of Electrical and Information Engineering, Seoul National University of Science and Technology, Seoul, South Korea. Since January 2018, he has been an Associate Professor with the Department of Electrical Power and Machines Engineering, Faculty of Engineering, Tanta University (FE-TU). He is currently the Director of the Electric and Hybrid Electric Vehicles Technology Laboratory, FE-TU. He is a supervisor of many Ph.D. and M.Sc. thesis. He has published more than 35 scientific research articles. His current research interests include advanced control techniques, electric drive systems, electric and hybrid electric vehicles, model predictive control in electrical drive systems and power converters, hybrid energy storage systems HESS, and wind and PV renewable energy systems. He is a peer reviewer in many transactions and conferences.